PREDICTING ACTUAL LOAD DEMAND IN DISTRIBUTION SYSTEMS WITH
HIGH PV PENETRATION

A THESIS SUBMITTED TO
THE GRADUATE SCHOOL OF NATURAL AND APPLIED SCIENCES
OF
MIDDLE EAST TECHNICAL UNIVERSITY

BY

UFUK YILDIZ

IN PARTIAL FULFILLMENT OF THE REQUIREMENTS
FOR
THE DEGREE OF MASTER OF SCIENCE
IN
ELECTRICAL AND ELECTRONICS ENGINEERING

SEPTEMBER 2019

Approval of the thesis:

PREDICTING ACTUAL LOAD DEMAND IN DISTRIBUTION SYSTEMS WITH HIGH PV PENETRATION

submitted by **UFUK YILDIZ** in partial fulfillment of the requirements for the degree of **Master of Science in Electrical and Electronics Engineering Department, Middle East Technical University** by,

Prof. Dr. Halil Kalıpçılar
Dean, Graduate School of **Natural and Applied Sciences**   _____

Prof. Dr. İlkay Ulusoy
Head of Department, **Electrical and Electronics Eng.**   _____

Assoc. Prof. Dr. Murat Göl
Supervisor, **Electrical and Electronics Eng., METU**   _____

Examining Committee Members:

Prof. Dr. A. Nezih Güven
Electrical and Electronics Eng., METU   _____

Assoc. Prof. Dr. Murat Göl
Electrical and Electronics Eng., METU   _____

Prof. Dr. Umut Orguner
Electrical and Electronics Eng., METU   _____

Assist. Prof. Dr. Ozan Keysan
Electrical and Electronics Eng., METU   _____

Prof. Dr. M. Timur Aydemir
Electrical and Electronics Eng., Gazi University   _____

Date: 06.09.2019

I hereby declare that all information in this document has been obtained and presented in accordance with academic rules and ethical conduct. I also declare that, as required by these rules and conduct, I have fully cited and referenced all material and results that are not original to this work.

Name, Surname: Ufuk Yıldız

Signature:

ABSTRACT

**PREDICTING ACTUAL LOAD DEMAND IN DISTRIBUTION SYSTEMS
WITH HIGH PV PENETRATION**

Yıldız, Ufuk
Master of Science, Electrical and Electronics Engineering
Supervisor: Assoc. Prof. Dr. Murat Göl

September 2019, 74 pages

Because of the increasing environmental concerns, governmental incentives and developing photovoltaic (PV) technology, PV systems have become increasingly popular in recent years. Despite the environmental and economic benefits of PV systems, installation of high number of PV systems brings new challenges in power system operation and management. Due to high number of PV systems at low voltage distribution systems and the computational load of communication and data analysis, the amount of power generated by these systems cannot be monitored. Therefore, it creates operational difficulties for the supply and demand balance for power system operators.

The load demand estimation methods currently used by the electricity grid operators cannot provide enough performance for systems with high number of PV systems. The main reason for this is that although the demand for load depends on social and economic conditions, solar energy production varies depending on geographical and climatic conditions. In order to provide better results, the generation data of each PV system should be obtained. As can be expected, monitoring all PV systems individually will be very costly.

This thesis aims to predict actual load demand in distribution systems with high PV penetration by predicting total solar power generation. The proposed method uses a small number of measurements and probabilistic knowledge on cloudiness over a city.

Numerical simulations for the methodology are provided based on measurements taken from several points in Ankara, Turkey. Numerical results prove that the accuracy of the proposed methods for the actual load demand prediction is getting better when total solar power generation is predicted by methodology stated in this thesis.

Keywords: Photovoltaic System, PV Generation Prediction, Actual Load Demand, Load Demand Prediction, Kalman Filter

ÖZ

ALÇAK GERİLİM GÜNEŞ ENERJİSİ SİSTEMLERİNİN VARLIĞINDA YÜK TALEP TAHMİNİ

Yıldız, Ufuk
Yüksek Lisans, Elektrik ve Elektronik Mühendisliği
Tez Danışmanı: Doç. Dr. Murat Göl

Eylül 2019, 74 sayfa

Artan çevresel kaygılar, devletin verdiği teşvikler ve gelişmekte olan fotovoltaik (PV) teknolojisi ile birlikte elektrik sistemlerindeki PV sistemler son yıllarda giderek daha popüler hale gelmiştir. PV sistemlerin çevresel ve ekonomik faydalarına rağmen çok sayıda PV sisteminin kurulması elektrik dağıtım şebekelerinin işletimi ve yönetiminde yeni zorluklar doğurmaktadır. Alçak gerilim dağıtım sistemlerinde güneş enerjisi sistemlerinin sayılarının fazlalığı ve iletişim ile veri analizinin hesapsal yükünden dolayı, bu sistemlerde üretilen enerji miktarı izlenememektedir. Dolayısıyla elektrik şebekesi operatörleri için arz talep dengesinin sağlanması adına operasyonel zorluklar yaratmaktadır.

Hali hazırda elektrik şebekesi tarafından kullanılan yük talep tahmin metotları alçak gerilim güneş enerjisi üretiminin fazla olduğu sistemler için yeterli performansı gösterememektedir. Bu yetersizliğin başlıca sebebi yük talebinin sosyal ve ekonomik koşullara bağlı olmasına rağmen, güneş enerjisi üretiminin coğrafi ve iklimsel koşullara bağlı olarak değişmesidir. Kullanılan metotların daha iyi sonuç verebilmesi için her güneş enerjisi panelinin üretim verisinin alınması gerekmektedir. Tahmin edilebileceği gibi bu çözüm oldukça maliyetlidir.

Bu çalışma kapsamında az miktarda farklı yerden alınan gerçek zamanlı ölçümler ile alçak gerilim güneş enerji panellerinin bölgesel üretimleri için matematiksel modeller oluşturulup tahminler yapılarak doğruluk oranı daha yüksek yük talep tahminlerinin elde edilmesi amaçlanmaktadır.

Sayısal sonuçlar Türkiye'nin Ankara ilinin birkaç noktasından alınan ölçümlere dayanarak elde edilmiştir. Elde edilen sonuçlar toplam güneş enerjisi üretimi için bu tezde belirtilen metot ile tahmin yapıldığında gerçek yük talep tahmini için önerilen yöntemlerin doğruluğunun arttığını kanıtlamaktadır.

Anahtar Kelimeler: Fotovoltaik Sistem, PV Üretim Tahmini, Gerçek Yük Talebi, Yük Talep Tahmini, Kalman Filtresi

To my family

ACKNOWLEDGEMENTS

TABLE OF CONTENTS

LIST OF TABLES

TABLES

LIST OF FIGURES

FIGURES

LIST OF ABBREVIATIONS

ABBREVIATIONS

ANN	Artificial Neural Network
ARIMA	Autoregressive Integrated Moving Average
ARMA	Autoregressive Moving Average
BTM	Behind-the-Meter
CFS	Correlation-Based Feature Selection
DRMSE	Daily Root Mean Square
GWp	Giga-Watt-Peak
kW	Kilo-Watt
kWp	Kilo-Watt-Peak
LV	Low Voltage
MLP	Multi-Layer Perceptron
MV	Medium Voltage
MW	Mega-Watt
MWp	Mega-Watt-Peak
PCA	Principle Component Analysis
PV	Photovoltaic
RMS	Root Mean Square
SVM	Support Vector Machine
SVR	Support Vector Regression
WNM	Wavelet Neural Networks

CHAPTER 1

INTRODUCTION

The importance given to renewable energy sources and as a result of this, the contribution of power generation by renewable energy, particularly PV systems, to electricity supply is constantly increasing day by day over the world as can be seen in Fig. 1-1 thanks to the increasing environmental concerns, governmental incentives and the decreasing cost of PV systems with technical improvements.
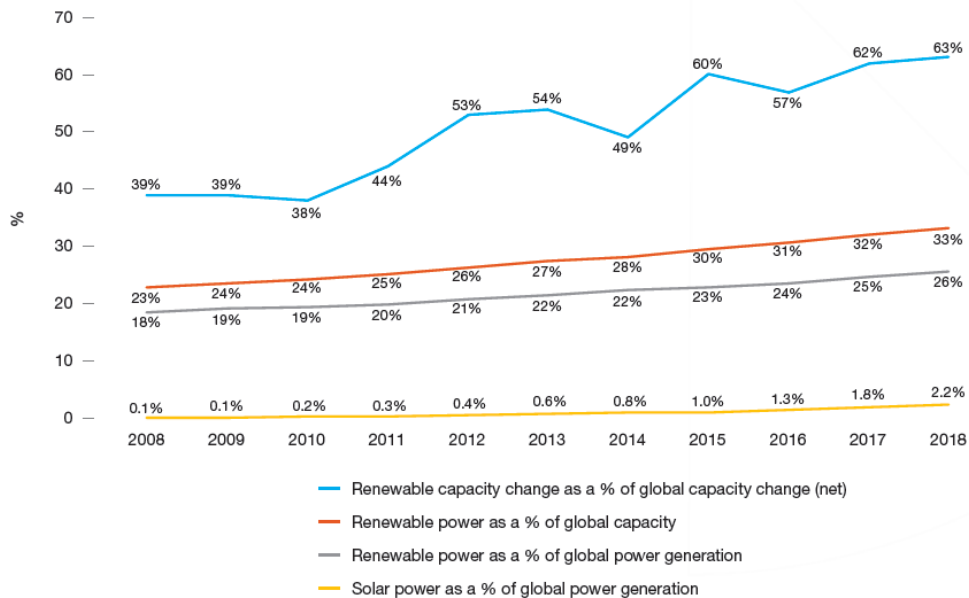
Figure 1-1. Renewable Power Generation and Capacity as a Share of Global Power 2008-2018 [1]

The rate of current solar developments is continuously increasing. As an important milestone, grid-connected solar power capacity reached 100 GW in 2016. In 2017, total of 99.1 GW of grid-connected PV systems were installed which was almost 30%

over the year-on-year growth of previous year as shown in Fig. 1-2 [1]. Also, that was almost equal to total capacity the world had in 2012.
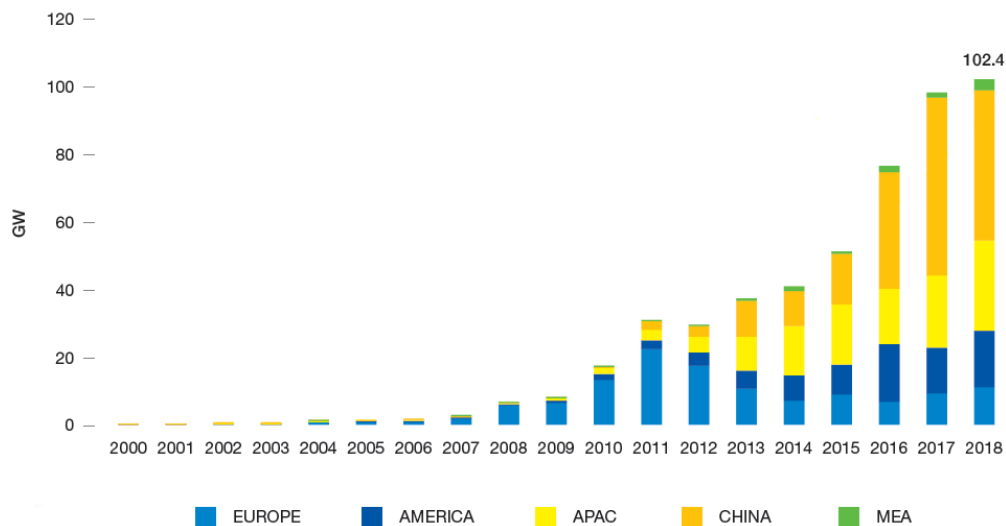
Figure 1-2. Evaluation of Global Annual Solar PV Installed Capacity 2000-2018 [1]

Accordingly, total global solar power capacity broke the 400 GW threshold in 2017 after it exceeded the 300 GW level in 2016 and the 200 GW level in 2015. In 2018, annual installation of solar power passed 100 GW level and total global solar power capacity reached 500 GWp or 0.5 TWp as shown in Fig. 1-3 [1].
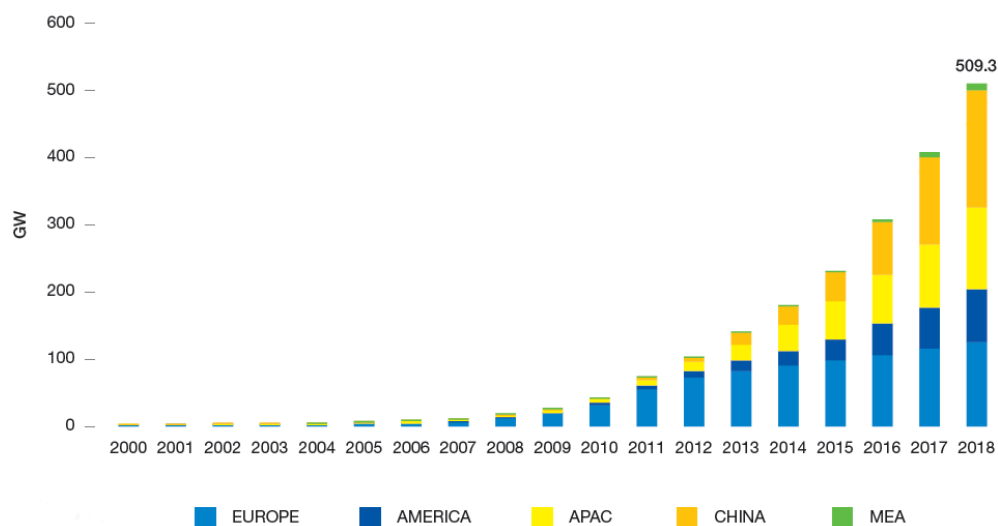
Figure 1-3. Global Total Solar PV Installed Capacity 2000-2018 [1]

The increase in solar power capacity is a consequence of the significant decrease in the cost of PV modules which continues to decrease as shown in Fig. 1-4 [1]. In February 2018, the lowest solar power price was recorded as a new world record with 2.34 US cents/kWh in Saudi Arabia [1].
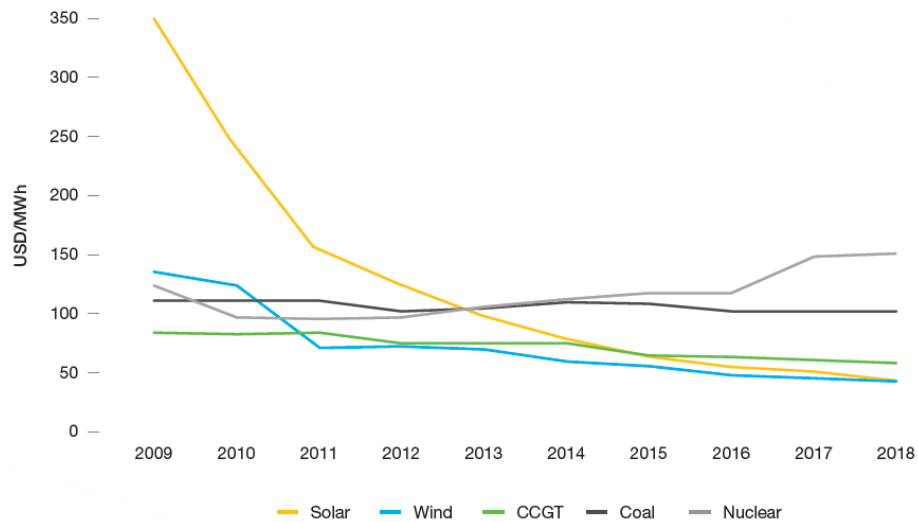
Figure 1-4. Solar Electricity Generation Cost in Comparison with Other Power Resources 2009-2018 [1]

In addition to its environmental and economic benefits, the installation of large amount of PV systems injects additional uncertainties in power system operation for utilities and system operators. One of the important effects of high penetration of PV systems is that forecast of electricity demand becomes less reliable. Electricity demand forecasting area is quite mature in the literature. Although the theories are well-developed, all of those methods require proper sets of data. The distribution system operators have been collecting electricity demand data however, measurements are only available at the HV/MV transformer substation. As the number of low voltage PV systems increases, the collected data become related to the net demand rather than actual demand. Fig. 1-5 shows the change in daily load curve with PV integration for fair and cloudy days. The area represented by blue color indicates net power demand from the grid and the area represented by yellow color indicates the power demand met by solar power generated by PV systems.
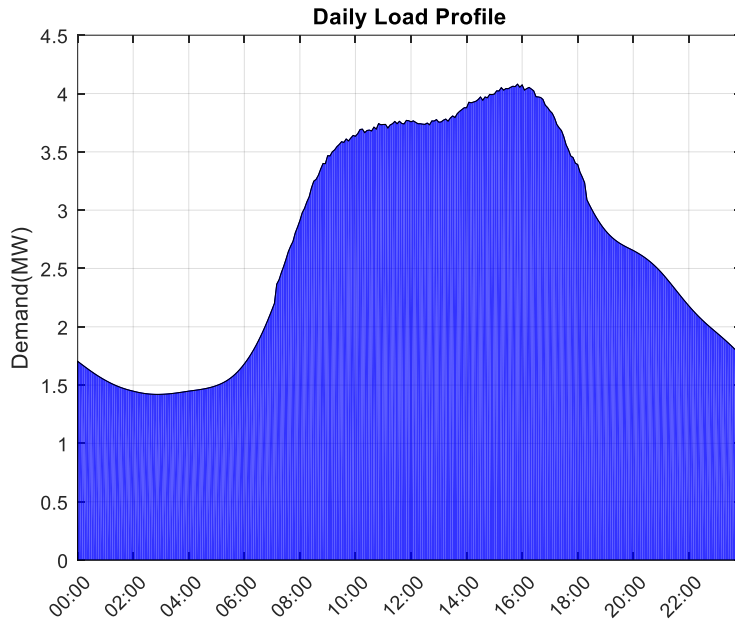
(a) Daily Load Profile without PV Integration
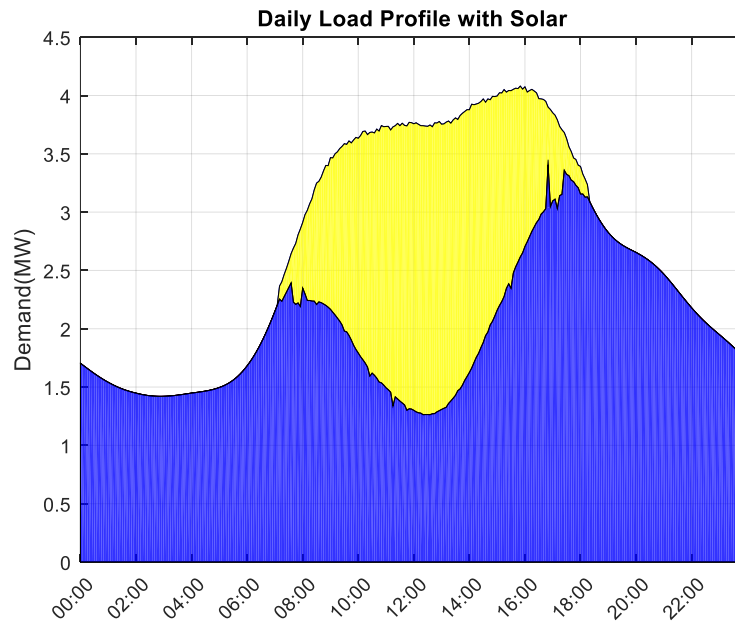
(b) Daily Load Profile with PV Integration for a Fair Day

Daily Load Profile with Solar
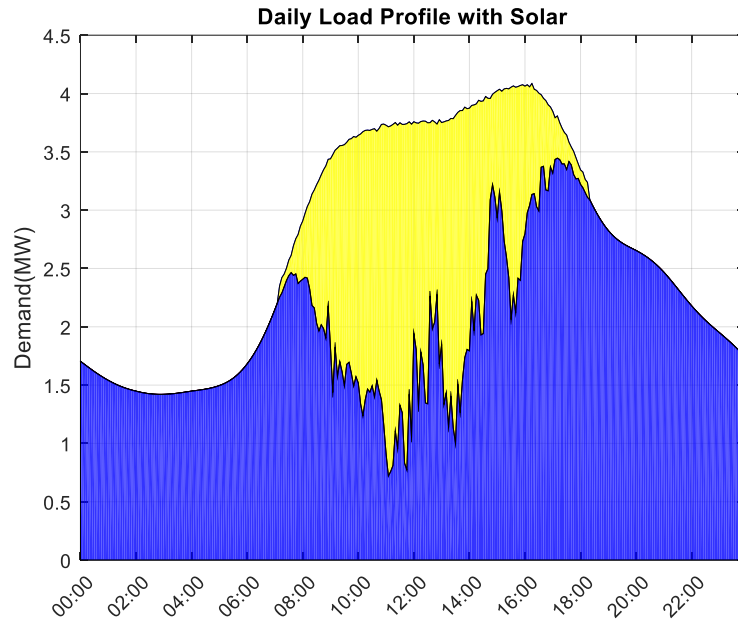
(c) Daily Load Profile with PV Integration for a Cloudy Day

Figure 1-5. Daily Load Profiles

In order to maintain proper system operation, actual demand should be known. Especially day-ahead decisions on market and system operation requires actual demand forecast of the upcoming day. Considering that the electricity demand characteristic is almost independent of solar power generation, as demand is affected mostly by the socio-economic and human factors while solar power generation is related to weather conditions, forecast of the actual demand becomes cumbersome as the PV systems populate. In order to forecast the actual demand, net electricity demand and solar power generation should be forecasted separately. However, an exact determination of the total solar power generation is not possible in today's distribution systems. Building an infrastructure to monitor, collect, archive and manage solar power generation data for every small-scale low voltage PV system would be very costly and computationally expensive. Even if there are methods for forecasting solar power generation, they rely on the weather forecast [2-4]. Although the weather forecasts have low resolution, because of the uncertainty in the cloudiness, pretty accurate forecasts can be performed for centralized PV systems connected to medium

voltage or high voltage power systems. However, because of the small sizes of the roof-top systems, the forecast accuracy drops for low voltage PV systems. Note that, effect of a single roof-top system is negligible however, in cities with high roof-top PV penetration, this decreased accuracy will end up with a significant uncertainty of power generation amount. Even if the ground-mounted PV systems are dominant in the solar market, rooftop PV systems have a great potential in the mid- to long-term as shown in Fig. 1-6.
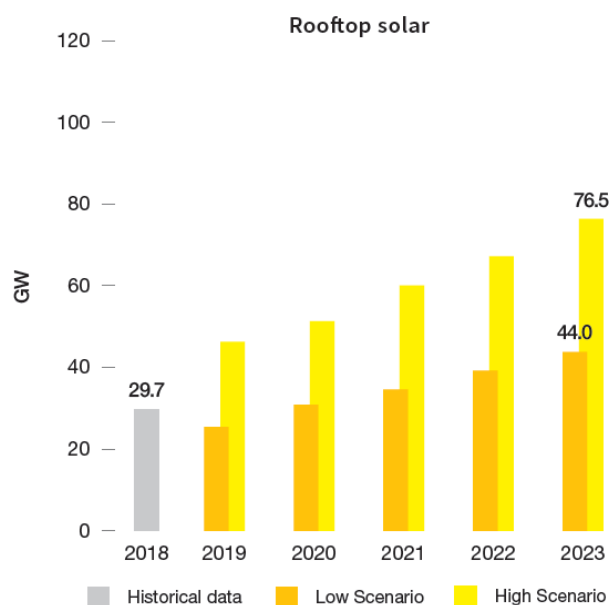
Figure 1-6. Scenarios for Solar PV Rooftop Development 2019-2023 [1]

This thesis proposes a method to predict actual load demand based on the prediction of the total solar power generation at a certain geographic area with a small number of monitored PV systems in order to improve situational awareness and provide an actual demand data with reduced bias.

1.1. Literature Review

In this section, literature reviews on total PV generation prediction and actual load demand prediction methods are provided.

1.1.1. Literature Review of Total PV Generation Prediction

Installation of PV system can be ground-mount or roof-top. Even if the ground-mounted PV systems constitutes higher fraction of the total PV systems installed, number of roof-top PV systems has already reached significant amount, and it is expected to increase further in the near future as can be seen in Fig. 1-6. Roof-top PV systems are normally located behind-the-meter (BTM) and invisible to system operators. BTM PV system is a PV system that generates power in order to use at the building that the system is installed, and its generation is not monitored and not known by the system operators. This unknown power generation brings new challenges to power system operation, and hence researchers started to pay attention to predicting BTM solar power generation. Although PV generation forecasting area is quite mature and several papers were published to review existing studies [2-5], the literature on predicting BTM solar power generation is still very limited.

In [6], a data-driven method based on dimension reduction and mapping functions is proposed to estimate the power generation of BTM PV by using a small number of representative PV systems and assuming the capacities of PV systems are already known. Proposed methodology is composed of four stages. In first stage, solar power generation data and any other available information are collected from the available sites within the area of interest over a limited time. In second stage, data dimension reduction is applied in order to obtain smaller subset of available information that represents same as all information acquired in first stage and get rid of unnecessary information. In third stage, mapping function is built that maps the total power generation from all PV systems to the information from subset of available information which are obtained in previous stage. Finally, the generation from all PV systems are predicted by using subset of information which is decided in second stage and mapping function built in third stage. Shaker et al. implemented five data dimension reduction techniques, namely, Principal Component Analysis (PCA), k-means Clustering, a proposed hybrid k-means+PCA approach, Relief, and Correlation-based Feature Selection (CFS) and four mapping functions, namely,

7

Linear Regression, Kalman Filter, Multi-Layer Perceptrons (MLP) and Wavelet Neural Networks (WNM). The methodology was evaluated using the PV generation data of California's power system with a total of 405 sites. The results showed that accuracy changes according to both data dimension reduction technique and mapping function employed, and they were provided with daily root mean squared error (DRMSE). Hybrid k-means + PCA approach with Linear Regression gave best prediction with DRMSE between 553kW and 65kW and representative PV systems between 2 and 30. When number of representative PV systems increases, the accuracy is getting better and DRMSE decreases for all techniques as expected.

In [7], the methodology is proposed based on the work in [6] by the same researchers. Previous work is improved by adding new features. In this work, uncertainty associated with the predicted power generation is also provided. This model does not need the historical information unlike in [6]. Since the model updates parameters continuously, it can easily adopt the future growth of capacity of BTM PV systems. Also, it relies on data from a limited number of sites. The methodology starts with selecting subset of PV systems within the specified sub-regions. The fuzzy numbers associated with each sub-region are developed by using information acquired from selected PV systems. Then, a small number of representative PV systems are chosen, and their real time power generation is used as the inputs of the model. Finally, the model calculates a fuzzy number associated with the real time power generation from all the PV systems within the region based on the existing BTM PV capacity of each sub-region. In this work, no numerical result was given for model accuracy.

1.1.2. Literature Review of Actual Load Demand Prediction

A large number of methods for load demand forecasting have been proposed in literature. They can be categorized into statistical methods and artificial intelligence methods. Mostly used statistical methods are linear regression [8-10], multiple linear regression [11,12], autoregressive moving average methods (ARMA) [13], autoregressive integrated moving average methods (ARIMA) [14], exponential

8

smoothing [15,16] and Kalman filter [17]. Some of frequently used artificial intelligence methods are artificial neural networks (ANN) [18-20], support vector machine (SVM) [21-23], genetic algorithm [24] and fuzzy logic [25].

These methods forecast the net load demand, rather than the actual load demand. In recent years, researchers started to devote more efforts to forecast actual load demand.

In [26], A. Kaur et al. aims to obtain actual load forecasting methodology for micro grids with high PV penetration. They implemented methodology in two different approach such that integrated and additive model. Solar power is forecasted based on clear sky model and load demand is forecasted by using different methods namely, autoregressive model, autoregressive model with exogenous input and support vector regression (SVR). For additive actual load forecasting, solar power and load demand are forecasted individually and then combined at the end. On the other hand, for integrated net load forecasting, where the solar power forecast is used as one of the input parameters for the load forecast model. The results showed that integrated model gives better results than additive model in terms of all error metrics.

In [27], classical neural network-based model is implemented to analyze impact the penetration of PV systems on load forecasting. They proposed the power penetration index that represent the amount of the penetration of PV systems to the distribution system. They have trained their model for different amount of PV penetration by changing power penetration index and obtained load forecasting results. They stated that proposed method is effective in improving the accuracy for load forecasting.

In [28], probabilistic actual load demand forecasting method was proposed considering a high BTM PV penetration. The idea of the proposed method is to extract the PV generation from the net load demand and then to forecast the actual load demand more accurate.

1.2. Thesis Outline

This thesis consists of five chapters. In the first chapter, motivation for this thesis is introduced. The reasons and effects of the high PV penetration to electricity grid in the world is discussed.

Chapter 2 provides a detailed description of photovoltaic effect, solar irradiance, PV cells, modules, arrays, systems and types of PV systems. The story of photovoltaics, how it all began and concept of it are explained. Solar irradiance which is the main source of photovoltaic effect and PV generation are examined. Also, what is PV cell and what is difference between cell, module, array and system are described, and types of PV systems are added. Additionally, bivariate normal distribution which will be the algorithm for predicting BTM PV generation is explained. Finally, Kalman filtering that will be used for prediction actual load demand is also summarized.

Chapter 3 introduces the proposed methods. First, the proposed method to predict total solar power generated by BTM PV systems in considered area is explained. Then, the proposed method to predict actual load demand that takes BTM solar power generation into consideration is presented.

Chapter 4 focuses on the tests which are done to evaluate proposed methods. Method proposed for prediction of total solar power generated in considered area is tested individually based on the solar radiation data collected in the city of Ankara, Turkey. Method proposed for the prediction of actual load demand is demonstrated on IEEE 33 Bus Distribution network by using the system data and the solar radiation data collected to evaluate the proposed method.

Chapter 5 summarizes the main contributions achieved throughout the thesis studies and possible future works.

CHAPTER 2

BACKGROUND REVIEW

This chapter introduces the technical background, which will conduce the reader understand the presented study. Firstly, PV systems will be explained. Then, impacts of high PV penetration on distribution system will be provided. Finally, basics of bivariate normal distribution and Kalman filtering will be introduced.

2.1. PV Systems

PV system is a power system designed to convert light energy directly into electricity. It is a clean, quiet and reliable way of generating electricity. Since the source of light is usually the sun, they are also called solar power systems. A summary of related topics to PV systems is provided next.

2.1.1. Photovoltaic Effect

The photovoltaic effect is the basic physical process of creation of electric current in a material when it is exposed to light. Sunlight consists of photons, and these photons contain different amounts of energies. When photons strike a PV cell, they may be reflected or absorbed. The energy of absorbed photon is transferred to an electron in an atom of the material. Electron can escape from its normal position to become part of the current in an electrical circuit with its newfound energy [29]. It is demonstrated in Fig. 2-1.
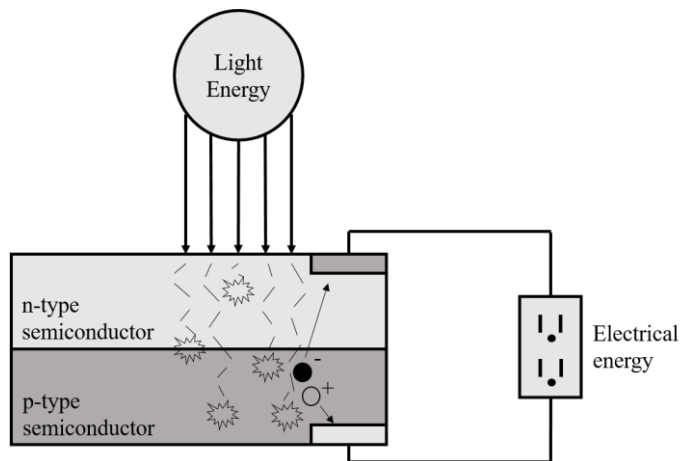
Figure 2-1. Photovoltaic Effect

The photovoltaic effect was first described in 1839 by French physicist Edmond Becquerel. He found that certain materials would produce small amount of electric current when exposed to light. He placed two coated platinum electrodes in a container with an electrolyte and observed the current flowing between them when exposed to light [29]. Becquerel's experiment can be illustrated as in Fig. 2-2.
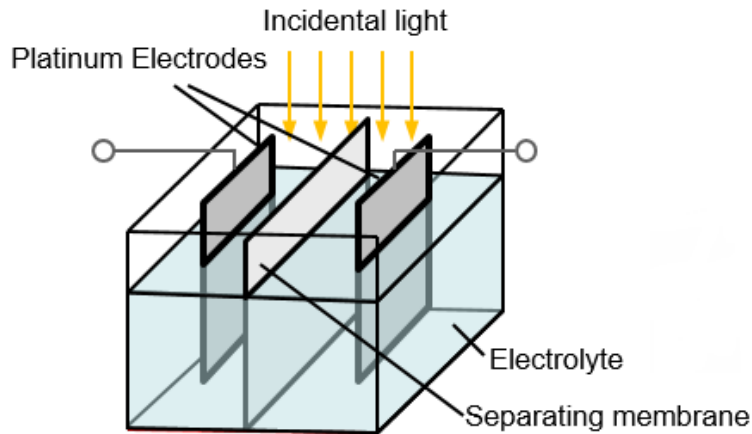
Figure 2-2. Illustration of Becquerel's experiment [30]

The next significant photovoltaic development was observation of William Adams and Richard Evans Day. They found out that a selenium rod provided with platinum electrodes can produce electrical energy when it is exposed to light. This is the first

time for that it was proven that a solid body can directly convert light energy into electrical energy [30].
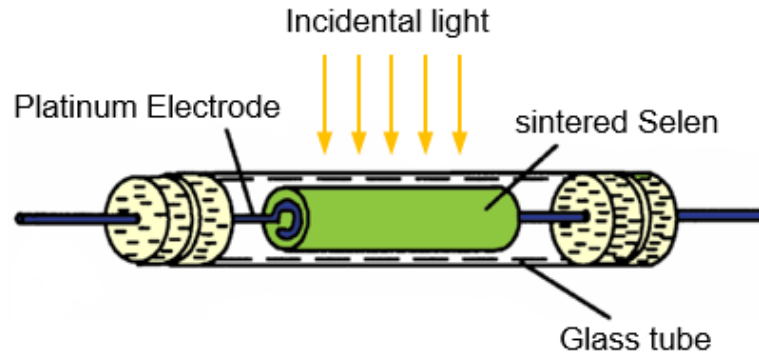
Figure 2-3. Sample geometry used by Adams and Day [30]

Major improvements for commercializing PV was taken in the 1940s and early 1950s after the Czochralski developed a process for producing highly pure crystalline silicon. This greatly increases the efficiency of silicon-based cells. In 1954, the first viable silicon PV cells are developed by Bell Laboratories scientists. This is the first solar cell which can convert enough of the sun's energy into power to run every day electrical equipment [29].

2.1.2. Solar Irradiance

Solar irradiance is the power received from the sun per unit area in the form of electromagnetic radiation. Since the main source of light is sun, solar irradiance has direct influence on the generation of PV system. Sunlight is radiated from the sun in all directions and starts to travel. When it reaches the atmosphere, its strength reduces to certain level. After it enters the atmosphere, its strength continues to decrease by scattering and absorbing by the clouds, dust and air molecules shown in Fig. 2-4. Sunlight that reaches the surface of PV modules without absorption and scattering is defined as direct solar radiation. Sunlight reflected by the ground is defined as reflected solar radiation. Sunlight scattered by the air molecules, dust etc. is defined as diffuse solar radiation.
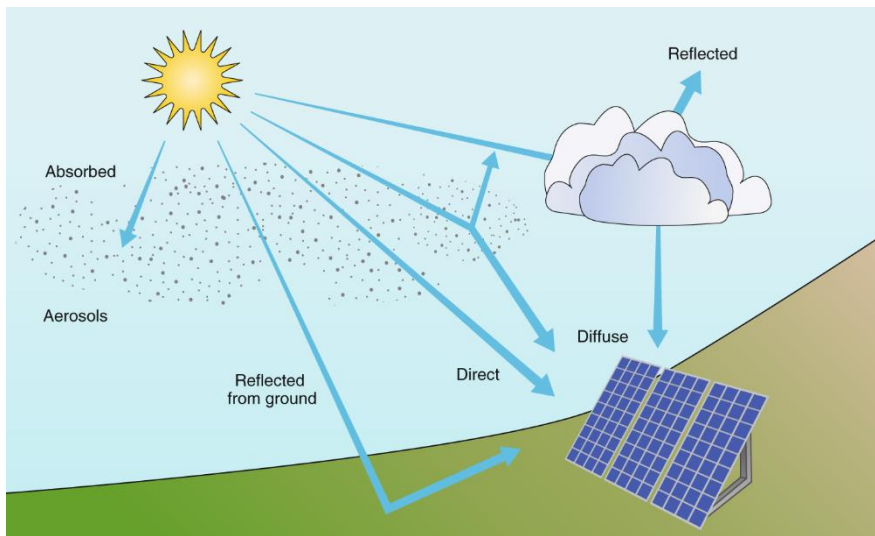
Figure 2-4. The path of solar radiation [31]

The strength of solar irradiance depends on the length of travel. Longer distance will result in weaker solar irradiance. Thus, polar regions will receive less solar irradiance because the sunlight needs to travel a longer distance to the polar regions. Global horizontal irradiation is the total irradiance from the sun on a horizontal surface of Earth can be seen in Fig. 2-5. It is the sum of direct irradiation and diffuse horizontal irradiation. Also, same map for Turkey where measurements are taken for test and evaluation can be seen in Fig. 2-6.
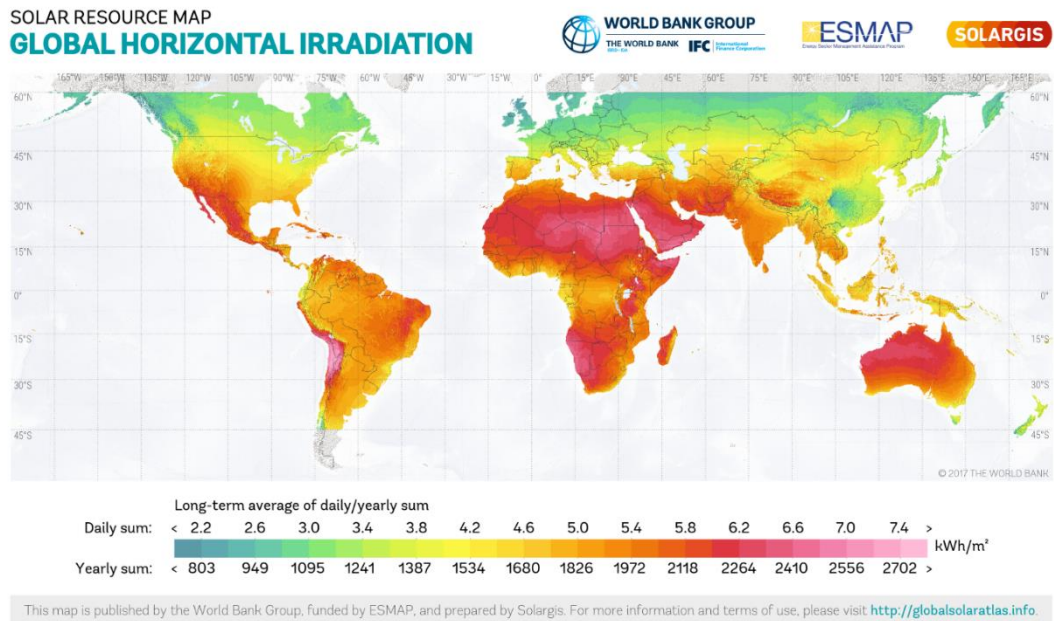
Figure 2-5. Global Horizontal Irradiation for World [32]
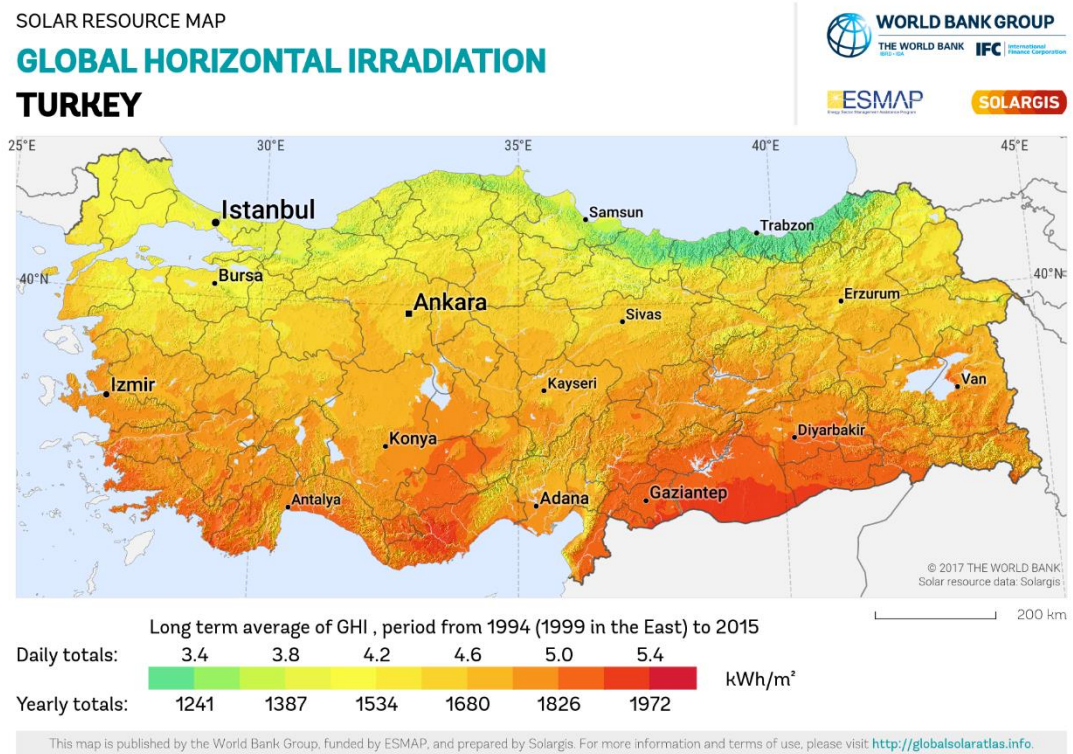
Figure 2-6. Global Horizontal Irradiation for Turkey [32]

This solar irradiance could be used as another form of energy. It can be captured by the solar collector which turn it into heat to provide hot water or heating in buildings. A large area of sunlight can be concentrated onto a small area by parabolic mirrors to acquire several thousand degrees Celsius. This heat can be used either for heating purposes or to generate electricity. Another way to make use of sunlight is to produce power from it by photovoltaic effect.

2.1.3. PV Cell

The basic unit in a PV system is PV cell which converts sunlight energy to electricity using semiconductor materials that exhibit the photovoltaic effect. Although many semiconductor materials are available, single-crystal silicon is the most popular for commercial cells since silicon is the second most abundant element in the Earth after oxygen. A conventional crystalline silicon PV cell can be seen in Fig. 2-7.

Figure 2-7. Single PV Cell [33]

PV cells are made of at least two layers of semiconductor material seen in Fig. 2-8. One layer has a positive charge, the other negative. When light strikes the cell, some of the photon from the light are absorbed by the semiconductor atoms, and the energy of absorbed atoms frees electrons from the cell's negative layer to flow through an external circuit and back into positive layer. This flow of electrons produces electric current.
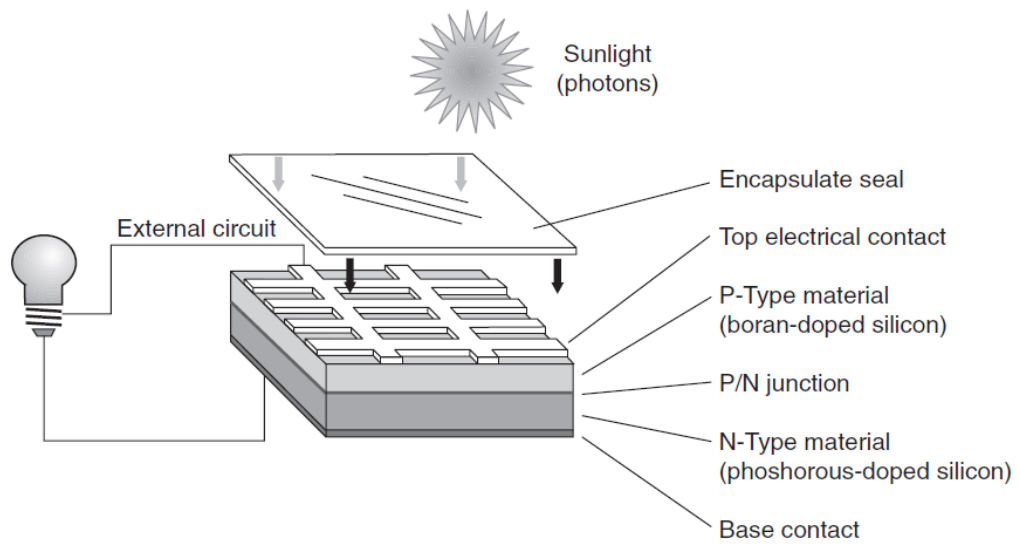
Figure 2-8. Basic Solar Cell Construction [34]

Ideal PV cells behave like a current source connected in a parallel with a diode. This model is completed with resistors to represents the losses. The most common circuits' equivalent to PV cell is shown in Fig. 2-9.
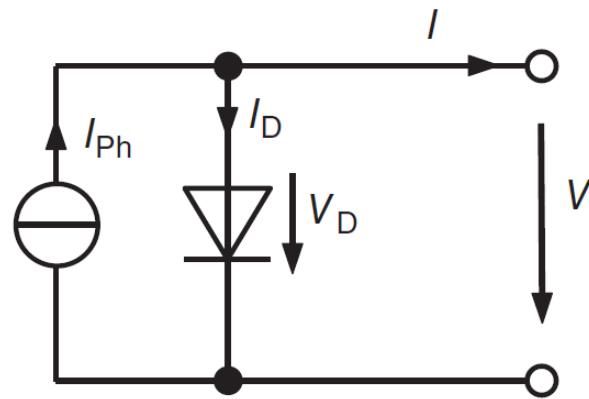
(a) Simplified Equivalent Circuit
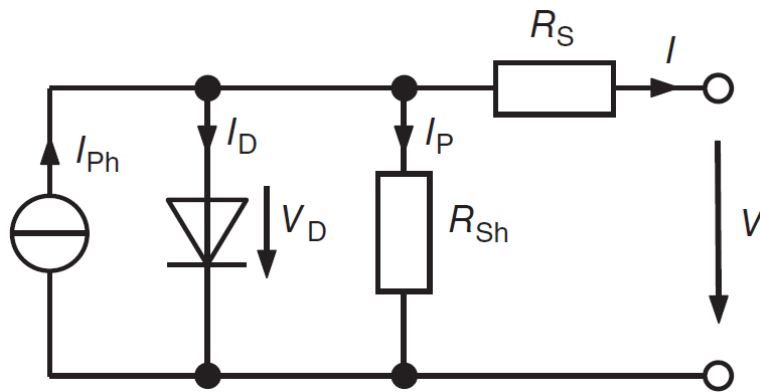
(b) Standard Equivalent Circuit
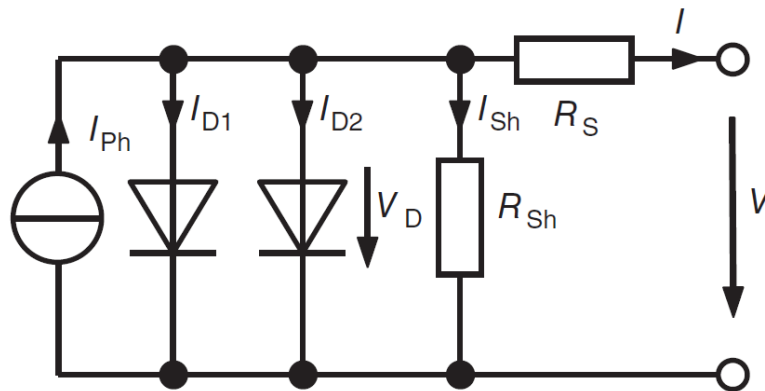
(c) The Two-diode Model

Figure 2-9. Equivalent circuits of PV cell [30]

PV cell produce DC current electricity and current times voltage equals to power, so I-V curves can be created to the current and voltage characteristics of a PV cell, module or array giving a detailed description of its solar energy conversion ability and efficiency. Fig. 2-10 shows I-V characteristics of a typical silicon PV cell operating under normal conditions.
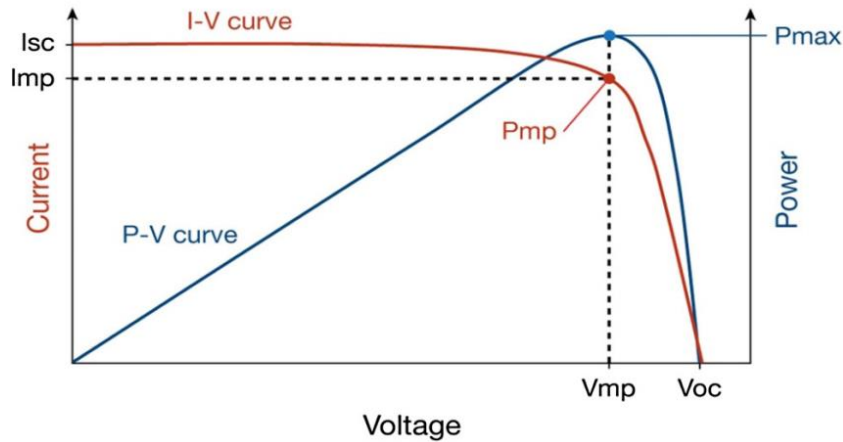
Figure 2-10. I-V Characteristics of a Typical Silicon PV Cell [35]

When the PV cell is open-circuited, the current will be at its minimum and the voltage across the cell at its maximum, known as the PV cells open circuit voltage, or Voc. When the PV cell is short-circuited, the voltage across the PV cell is at its minimum and the current flowing out of the cell reaches its maximum known as the PV cells short circuit current, or Isc.

PV cell can work from the short circuit current (Isc) at zero output volt, to zero current at the full open circuit voltage (Voc). However, there is one point which the power reaches its maximum value, at Imp and Vmp known as the PV cells maximum power point, or Mpp. Therefore, the ideal operation of PV cell is defined to be at the maximum power point.

However, capacity of power generation of single PV cell is limited. PV cells can be wired or connected in either series or parallel combinations, or both to increase its power generation capacity.

2.1.4. PV Modules, Arrays and Systems

The most basic part of a PV system is the cell. In order to increase produced electric current or power, lots of individual PV cells are interconnected together in a sealed, weatherproof package called a module. When two modules are wired together in series, their voltage is doubled while the current stays constant. When two modules are wired in parallel, their current is doubled while the voltage stays constant. To achieve the desired voltage and current, modules are wired in series and parallel into what is called a PV array shown in Fig. 2-11. The flexibility of the modular PV system allows designers to create solar power systems that can meet a wide variety of electrical needs, no matter how large or small.
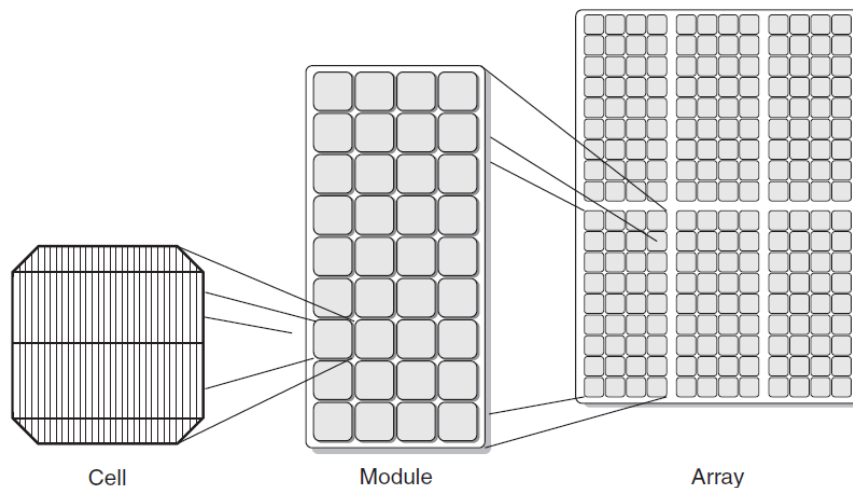
Figure 2-11. Photovoltaic Cell, Module and Array [34]

2.1.5. Types of PV Systems

2.1.5.1. Direct PV Systems

These are the simplest PV systems with the fewest components. They include only the PV module and the load. The DC output is immediately directed to DC loads. Because they do not have batteries and are not tied to the grid, they only power the loads when the sun is shining.

2.1.5.2. Off-Grid PV Systems

Off-grid PV systems, which are also called stand-alone PV systems can consist of the PV modules, load and batteries for energy storage as seen in Fig. 2-12. The power generated by PV modules is in the form of DC which feeds through a charge controller and is stored in the batteries when the power is needed it flows through and inverter to change it to AC for use in loads.
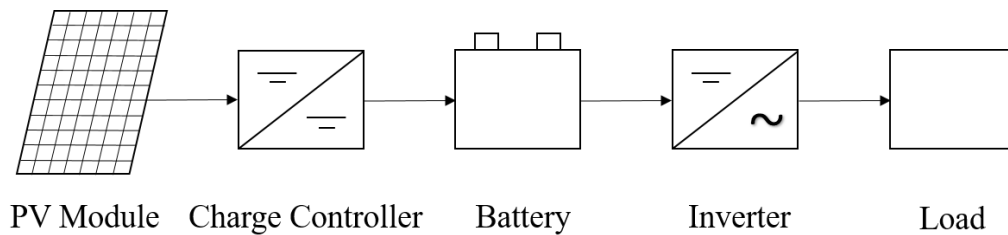
Figure 2-12. Typical Off-Grid PV System

2.1.5.3. Grid-Connected PV Systems

Grid-connected PV system is a PV system that is connected to the utility grid. Like off-grid PV system, grid-connected PV system consists of the PV module, inverter and loads as seen in Fig. 2-13. Unlike off-grid power systems, a grid-connected system rarely includes an integrated battery solution, as they are still very expensive. It additionally has grid-connection equipment. They range from small residential and commercial rooftop systems to large utility-scale solar power stations. When power is generated by the PV system in the form of DC that is converted to AC by the inverter and then used directly in property. When no power is being generated by the PV system, power is drawn from the grid. When possible, excess power generated by PV system can be back into the grid. Grid-connected PV systems in the world account for about 99% of the installed capacity compared to stand alone systems, which use batteries. Battery-less grid connected PV systems are cost effective and require less maintenance [36].
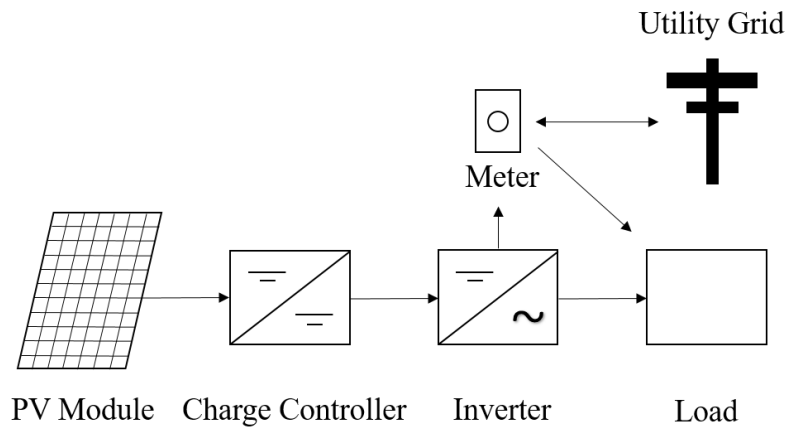
Figure 2-13. Typical Grid-Connected PV System

2.1.5.4. Hybrid PV Systems

Hybrid PV systems combine the off-grid and grid-connected PV systems. The hybrid system can be considered as off-grid solar with utility back-up power, or grid-connected solar includes battery back-up as seen in Fig. 2-14.
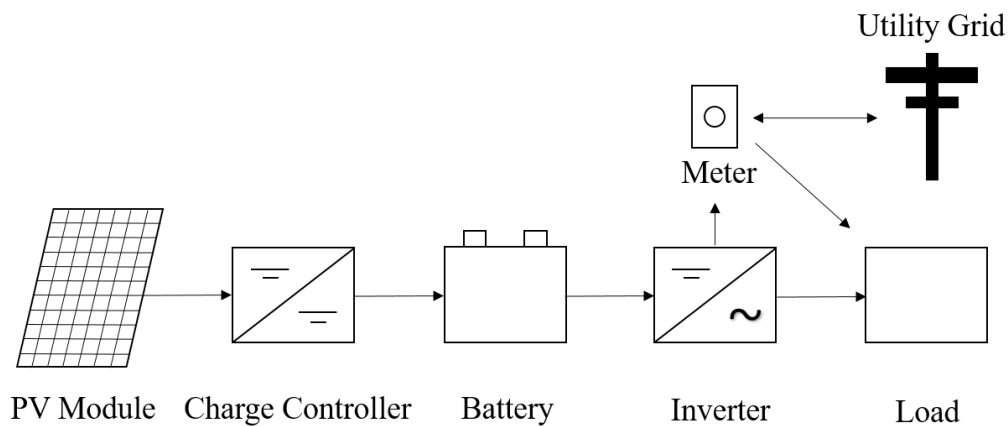
Figure 2-14. Typical Hybrid PV System

2.2. The Impacts of Increased PV Penetration on Distribution Systems

Solar PV systems look to be a good option for improving the performance of the power system. It can provide required power for increasing load and reduce the cost of the electricity prices. As the price of the solar PV decreases, the capacity of PV systems

increases accordingly. However, increased PV generation in distribution systems has several negative impacts on the distribution grid as well as positive impacts. Some of the important issues are related to voltage quality, power quality, harmonics and power balancing.

2.2.1. Voltage Quality

Large number of PV systems in distribution system can affect the voltage level of the system. Traditionally, in distribution systems the power flow is unidirectional from the medium voltage system to the low voltage systems. Thus, in normal operation, the current flows from distribution transformer to the loads, which results in voltage drops along the feeder line due to transformer and line impedances. There are some voltage regulation devices, such as step voltage regulators, on-load tap changing transformers, switched capacitors to compensate voltages because voltage level at load locations must be maintained within specified ranges for safe operation. However, when penetration of PV systems reaches significant level, there are moments when the generation is more than demand, especially in sunny days and at noon. As a result, the voltage at the Point of Common Coupling (PCC) of the inverter and grid increases. Therefore, direction of power flow changes and power starts to flow from PV systems to distribution transformer. This opposite direction of flow cause overloading of the distribution feeders and higher power losses. It also affects the operation of voltage regulators [37].

Voltage quality can also be affected by the additional variability associated with weather-dependent PV generation characteristic. PV generation could vary continuously due to variations in solar irradiance caused by the movement of clouds and resulting shadows.

2.2.2. Power Quality

PV systems are normally designed to supply only real power which means that PV inverters operate at unity power factor in order to increase the active power generated. If PV systems partially supply required power by the loads, active power supplied

from the utility will decrease. However, reactive power requirements are still the same and have to be supplied by the utility. This high rate of reactive power supply causes the system power factor to decrease. In this case, distribution transformers operate at low power factor. Efficiency of transformer decreases as their operating power factor decreases. This led to overall losses in distribution transformer increase which reduces the overall system efficiency.

2.2.3. Harmonics

When penetration of PV systems in distribution systems increases, the harmonic distortion of current and voltage waveform draws the attention. It is due to fact that PV inverters inject harmonics into the system during conversion of DC current to AC current in order to synchronize with the AC main supply. Although the inverters inject current harmonics into the system, they do not have significant impact on voltage harmonics [38]. If the high frequency harmonics produced by the inverters are not properly filtered, they mainly lead to increased losses in distribution system through heating. They also cause the stray and eddy current losses and reduce the transformers life due to increased temperature in the windings [39].

2.2.4. Power Balancing

With the increasing penetration of PV systems to the power system, extra effort has to be made in order to maintain supply-demand balance. When power injection from PV systems to the power system increases, the amount of power generation by conventional power generators should be reduced. Since PV generation could vary continuously due to variations in solar irradiance, achieving the balance of supply and demand could be challenging.

2.3. Bivariate Normal Distribution

The normal distribution, also called the Gaussian distribution and the bell curve, is a distribution that occurs naturally in many situations that describes how the values of variable are distributed. It is a symmetric distribution where most of the variables

group together around the central peak and the probabilities for values further away from the mean decrease equally in both directions. The general formula for the probability density function of the normal distribution is:

$$f(x) = \frac{1}{\sqrt{2\pi\sigma^2}} e^{-\frac{(x-\mu)^2}{2\sigma^2}} \qquad (2.1)$$

$$= \frac{1}{\sqrt{2\pi\sigma^2}} exp\left\{-\frac{(x-\mu)^2}{2\sigma^2}\right\} \qquad (2.2)$$

where,

μ is the mean or expectation of the random variable 'x',

σ is the standard deviation of the random variable 'x'.

The parameters for the normal distribution define its shape and probabilities entirely. The shape of it varies according to parameter values as shown in the Fig. 2-15.
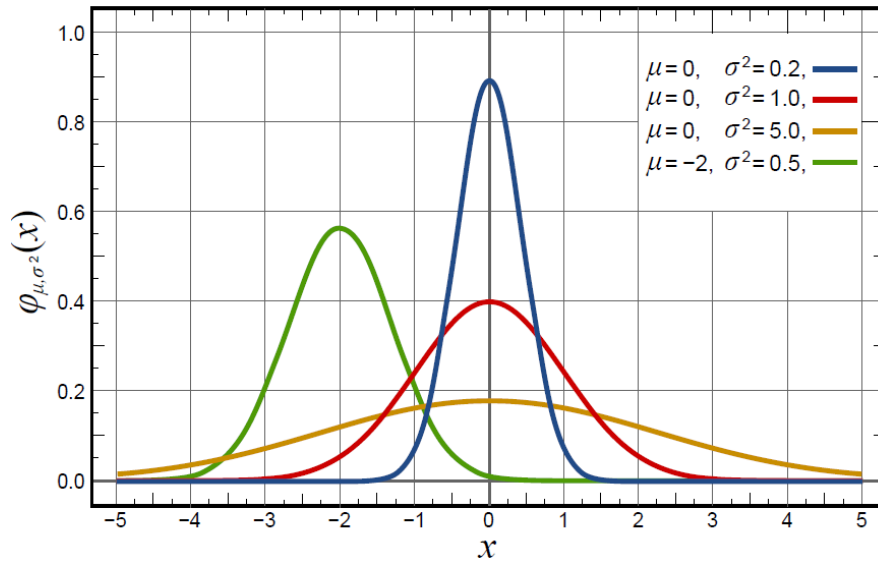
Figure 2-15. Normal Distributions [40]

The values group together around the mean. The standard deviation expresses how much the values differ from the mean. If the standard deviation is high, the values spread out and will be further from the mean.

The properties for the probability density function curve as follows,

• The total area under the normal curve represents the sum of all probabilities for a random variable and is equal to 1.

• The probability for a normal random variable X equals any specified value is 0.

• The probability for X is greater than any specified value x equals the area under the normal curve between x and plus infinity.

• The probability for X is less than any specified value x equals the area under the normal curve between x and minus infinity.

• The probability for X is between any specified value x and any specified value y equals the area under the normal curve between x and y.

For every normal distribution curve:

• Almost 68.2% of values falls within the mean and 1 standard deviation distance.

• Almost 95.6% of values falls within the mean and 2 standard deviation distance.

• Almost 99.8% of values falls within the mean and 3 standard deviation distance.

as stated in Fig. 2-16.
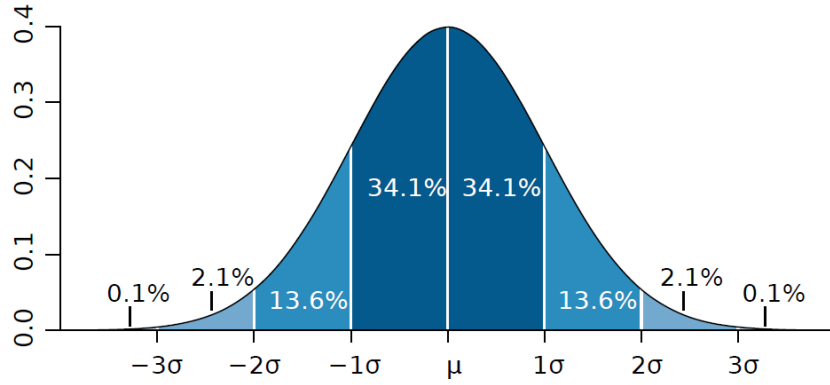
Figure 2-16. Probability of Normal Distribution [41]

Normal distribution of a single random variable is called univariate normal distribution. On the other hand, normal distribution of a group of random variables is called multivariate normal distribution. Bivariate normal distribution is a special case of the multivariate normal distribution and it is made up of two independent random variables.

Z and T are two independent normal random variables, and two other random variables X and Y of the form

$$X = aZ + bT, \tag{2.3}$$

$$Y = cZ + dT, \tag{2.4}$$

where a, b, c, d, are some scalars. Since they can be expressed as a linear function of independent normal random variable, X and Y are also normal. Moreover, since X and Y are linear functions of the same two independent normal random variables, their joint PDF takes a special form, known as the bivariate normal PDF.

For a given two variables $x, y \in \mathbb{R}$, the bivariate normal probability density function is,

$$f(x,y) = \frac{exp\left\{-\frac{1}{2(1-\rho^2)}\left[\frac{(x-\mu_x)^2}{\sigma_x{}^2} + \frac{(y-\mu_y)^2}{\sigma_y{}^2} - \frac{2\rho(x-\mu_x)(y-\mu_y)}{\sigma_x\sigma_y}\right]\right\}}{2\pi\sigma_x\sigma_y\sqrt{1-\rho^2}} \tag{2.5}$$

27

where,

$\mu_x \in \mathbb{R}$ and $\mu_y \in \mathbb{R}$ are the marginal means of random variables 'x' and 'y'

$\sigma_x \in \mathbb{R}^+$ and $\sigma_y \in \mathbb{R}^+$ are the marginal standard deviations of random variables 'x' and 'y'

$0 \leq |p| < 1$ is the correlation coefficient

X and Y are normally distributed and denoted as $X \sim N(\mu_X, \sigma_X{}^2)$ and $Y \sim N(\mu_y, \sigma_y{}^2)$
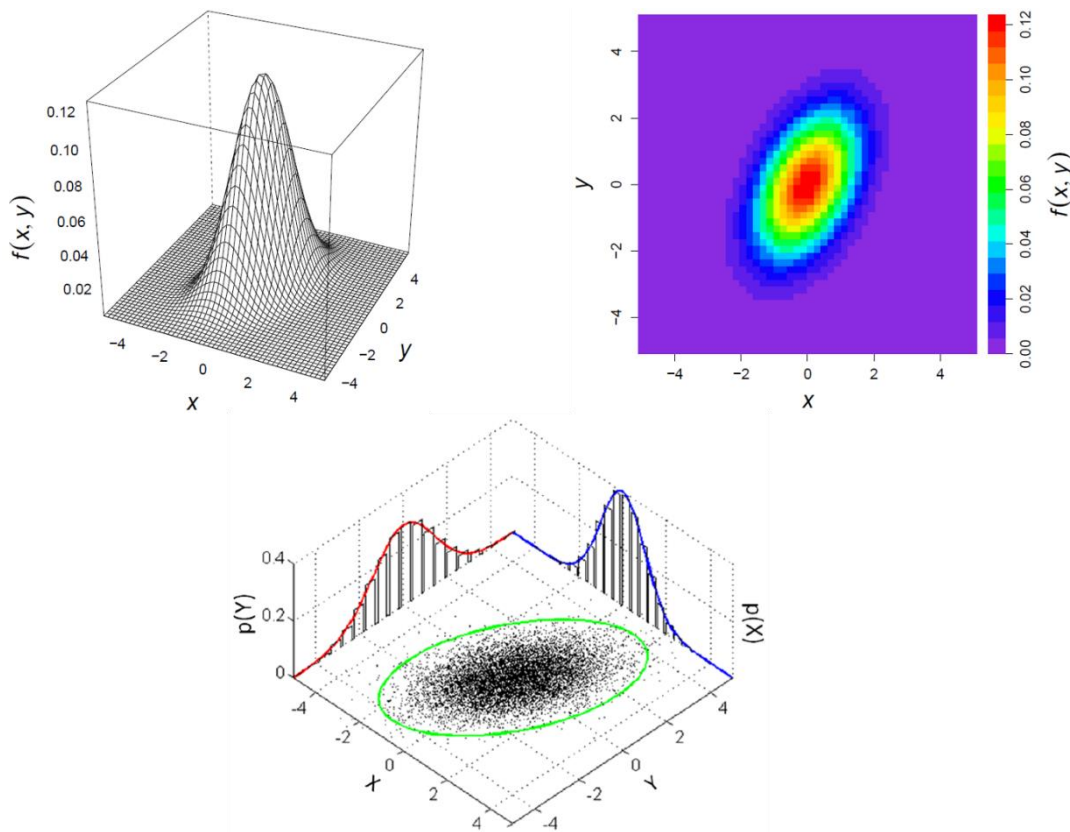
Figure 2-17. Bivariate Normal Distribution [42]

The bivariate normal PDF has several useful properties. In this work, property of the conditional distribution will be used. If a pair of X and Y has bivariate normal distribution, the conditional expectations $(X|Y)$ and $E(Y|X)$ will be a linear function of Y and X, respectively. The relationship can be described as follows:

$$E(Y|X) = E(Y) + \rho_{X,Y}.\sigma_Y \frac{X - E(X)}{\sigma_X} \qquad (2.6)$$

where $E(X)$ and $E(Y)$ are the expected values of X and Y, respectively, σ_X and σ_Y are the standard deviations of X and Y, respectively and $\rho_{X,Y}$ is the correlation coefficient.

2.4. Kalman Filter

Kalman filter which is also called 1inear quadratic estimator is a useful tool for a variety of different applications. It does what all filters do which is to let something pass through while something else does not. A Kalman filter sorts out the useful parts of information which have some error or noise and figures out what actually happened. It can be used in any place where there is uncertain information about some dynamic system.

An example diagram of Kalman filter can be seen in Fig. 2-18.
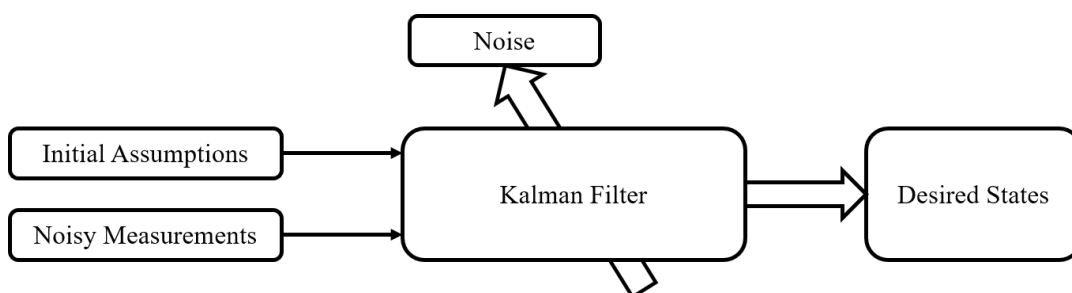
Figure 2-18. Diagram of Kalman Filter

Kalman filter is used to estimate states for linear dynamical systems in state space format, i.e.

$$x_k = F_{k-1}x_{k-1} + G_{k-1}u_{k-1} + w_{k-1} \qquad (2.7)$$

$$y_k = H_k x_k + v_k \qquad (2.8)$$

where,

x_k is the state vector at time instant k,

x_{k-1} is the state vector at time instant $k-1$,

y_k is the output vector at time instant k,

u_{k-1} is the input vector at time instant $k-1$,

w_{k-1} is the process noise vector at time instant $k-1$,

v_{k-1} is the measurement noise vector at time instant $k-1$,

F_{k-1} is the state system matrix at time instant $k-1$,

The state vector, x, are the values which will be tried to be estimated by the filter. The output vector, y, are the measurements. Measurements should be expressed in terms of the states. The input vector, u, can be any information which can help to define the system dynamics. The random variables, w and v, represents the process and measurement noise, respectively. They are assumed to be zero mean and used to determine the process and measurement noise covariance matrices Q and R. System matrices, F, G and H, contain the coefficients of the equations.

The Kalman filter is a recursive process which is composed of prediction followed by a correction. The all information about the state is used to project the filter forward and predict the next state. The process is started with initial estimate, $\hat{x}_0$, and initial state error covariance matrix, P_0, Kalman filter procedure is applied recursively at each time step. First, the state vector is predicted from the state dynamic equation using,

$$\hat{x}_{k|k-1} = F_{k-1}\hat{x}_{k-1} + G_{k-1}u_{k-1} \qquad (2.9)$$

where $\hat{x}_{k|k-1}$ is the predicted state vector before correction, $\hat{x}_{k-1}$ is the previous estimated state vector. Next, the state error covariance matrix is predicted using,

$$P_{k|k-1} = F_{k-1}P_{k-1}F^T{}_{k-1} + Q_{k-1} \qquad (2.10)$$

where $P_{k|k-1}$ is the predicted state error covariance matrix before correction, P_{k-1} is the previous estimated state error covariance matrix, and Q is the process noise covariance matrix. Once the predicted values are obtained, the Kalman gain matrix, K_k, is calculated using,

$$K_k = P_{k|k-1}H^T{}_k(H_kP_{k|k-1}H^T{}_k + R_k)^{-1} \qquad (2.11)$$

where H is a matrix necessary to define the output equation and R is the measurement noise matrix. The state vector is then updated by using the calculated Kalman gain matrix in order to correct the prediction by the appropriate amount, as in,

$$\hat{x}_k = \hat{x}_{k|k-1} + K_k(z_k - H_k\hat{x}_{k|k-1}) \qquad (2.12)$$

Similarly, the state error covariance is updated by,

$$P_k = (I - K_kH_k)P_{k|k-1} \qquad (2.13)$$

where I is an identity matrix.

Recursive operation of the Kalman filter can be seen in Fig. 2-19.
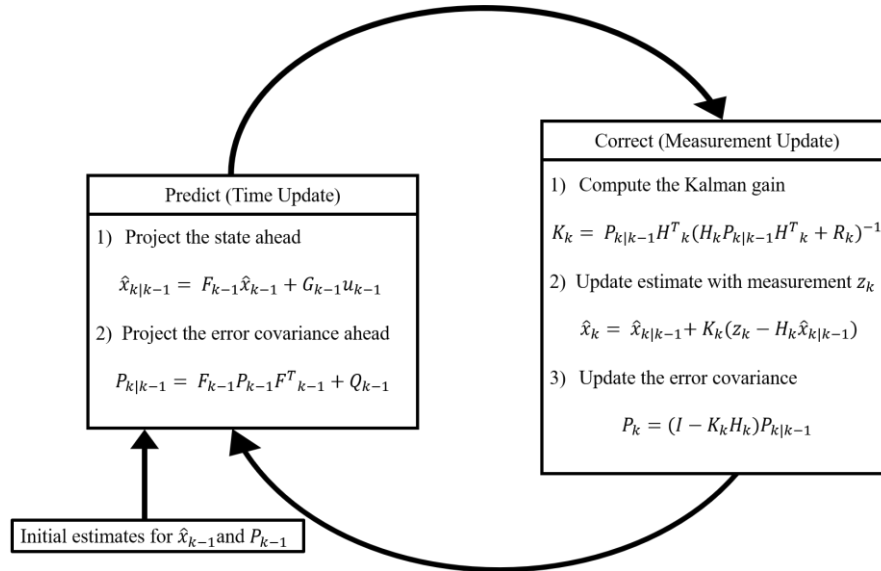
Figure 2-19. A recursive operation of the Kalman filter

CHAPTER 3

PROPOSED METHOD

After presenting the general introduction and detailed literature review in Chapter 1, required technical background for helping the reader to understand the concept is reviewed in Chapter 2. In this chapter, proposed methods will be explained. The proposed method aims to acquire actual load demand from measurements available at the HV/MV transformer substation and small number of PV systems generation measurements. It is proposed as a two-step method. First, total PV generation is obtained by predicting generation amounts of unmonitored PV systems. Then, actual load demand prediction is performed based on total PV generation prediction.

3.1. Total PV Generation Prediction

This section explains the proposed method for the prediction of solar power generated by BTM PV systems whose generations are not monitored continuously. The proposed method assumes,

- the rated power and location of every single PV system in considered area is known,
- factors affecting PV performance are almost same for each PV system in the considered area, such as;
    - PV cell material, e.g. silicon,
    - Global horizontal irradiation, which depends on latitude, season, time of day and altitude,
    - tilt angle,
    - ambient temperature.

Considering that many distribution system operators can collect information on the power-rating, cell-type and tilt angle while the meters at those locations are changed to four-quadrant meters, and the parameters affecting the PVE performance will not vary considerable across a city, the assumptions can be considered as realistic.

Power generation of PV systems is affected by several factors, but it is mostly determined by irradiation amount. The irradiation amount at different points in a city are related to the cloudiness of the sky. It is expected that cloudiness conditions of two close locations are more similar compared to more distant ones [43,44], such that their correlation is high. This constitutes the core of the proposed approach. As the distance between those two locations decreases, similarity between the cloudiness patterns observed at those locations increases. Therefore, one can use a representative PV system to predict total solar generation of the all other systems provided that the distances among the representative site and the other systems are limited. In a large city, utilization of a single representative site is not possible, therefore, the considered region should be divided into sub-regions. In order to divide the system into sub-regions, one may collect irradiation data from different points of the whole considered region, and then compare the correlation among the observed values corresponding to the same time. In this step, it is not required to collect data from every single PV system in the whole considered area. Irradiation data from some different points can be collected in order to obtain correlation between irradiation between two different points with respect to distance. If the correlation coefficient goes down below a certain value, that distance determines the radius of sub-region.

Once the sub-regions are determined, the proposed method collects data from the representative sites and predicts the total solar generation of the city based on the bivariate normal distribution.

The flow chart of the proposed method is presented in Fig. 3-1, and details of each step of the proposed method are presented in the following sub-sections.

34
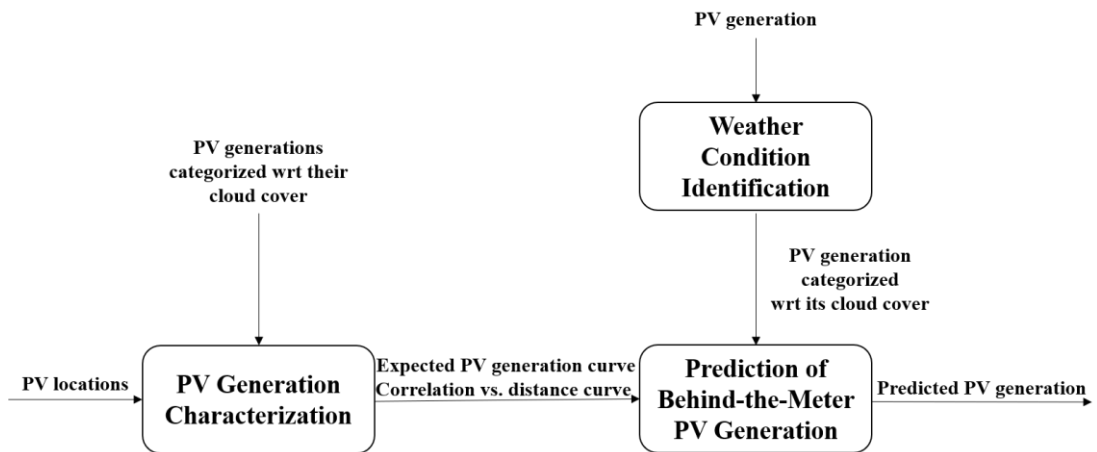
Figure 3-1. Flow Chart for Predicting Total Solar Power Generation

Step-1. PV Generation Characterization

This step is the offline modeling of the relation between the representative site and other PV systems in sub-region. Once the model is constructed, this step does not have to be reperformed. Note that, as the proposed modeling provides the relation between the representative site and any point in the sub-region, even if new PV systems are added, running this stage again will be redundant.

Distance between two PV systems and the cloudiness of the sky are the most significant factors that determines the probabilistic relation between generation amounts of those two PV systems. As the distance increases, the uncertainty between the generation amounts of the PV systems increases. Similarly, as the cloudiness level increases, the uncertainty increases as well. In order to obtain a probabilistic model of the relation between generation amounts of the any PV systems and the representative site, this study proposes to form correlation versus distance curves. Since correlation is also affected by cloudiness amount considerably, three curves are formed based on the cloudiness level of the sky, such that:

- Fair,
- Partly cloudy,
- Mostly cloudy.

One can model the relation between the representative site and other systems which are located at any point in the same sub-region based on the correlation, as shown below.

$$\rho_{X^w Y_d^w} = \frac{cov(X^w, Y_d^w)}{\sigma_{X^w} \sigma_{Y_d^w}} \tag{3.1}$$

where,

$\rho_{X^w Y_d^w}$ is the correlation between X^w and Y_d^w,

X^w is the solar radiation corresponding to the day type 'w' recorded at the representative site,

Y_d^w is the solar radiation corresponding to the day type 'w' recorded at location 'd ',

σ_{X^w} is the standard deviation of the solar radiation corresponding to the day type 'w' recorded at the representative site,

$\sigma_{Y_d^w}$ is the standard deviation of the solar radiation corresponding to the day type 'w' recorded at location 'd ',

w is the day type, such that w can be fair, partly cloudy or mostly cloudy.

In order to form the model, solar irradiation data from different points in a sub-region are collected. One of those points is the representative PV site. As the correlation between the generated power and solar irradiation is very high, one can collect power generation instead of solar radiation as well. Note that, this stage is offline and performed once. No communication infrastructure is required, rather mobile pyranometers or data recording energy analyzers can be used.

Fig. 3-2 presents sample regression curves for fair, partly cloudy and mostly cloudy weather conditions. The data used to form those curves were collected in the city of Ankara, Turkey by two different pyranometers. Every three points in different colors for same distance in this figure has been obtained after a month of data collected

36

period. During these periods, solar irradiation data has been continuously collected from representative PV site location by one of the pyranometer and for each period solar irradiation data has been collected from a point as far as the distance specified in the graph by other pyranometer. After obtaining solar irradiation data, they have been categorized into three groups as fair, partly cloudy and mostly cloudy according to weather conditions and correlation between two measurements from representative PV site location and from other points were calculated using (3.1). One can determine approximate value of the required correlation value corresponding to a location using those curves.
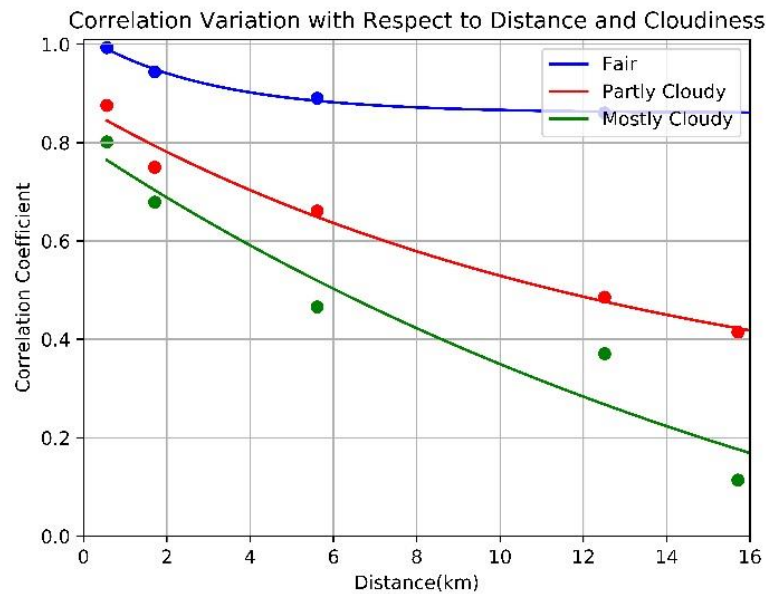
Figure 3-2. Correlation Variation with Respect to Distance and Cloudiness

Those curves show that there is a correlation between the power generations of PV systems within a certain area considerably up to 5km radius, and the amount of correlation changes according to the level of cloudiness as can be seen from closer in Fig. 3-3.
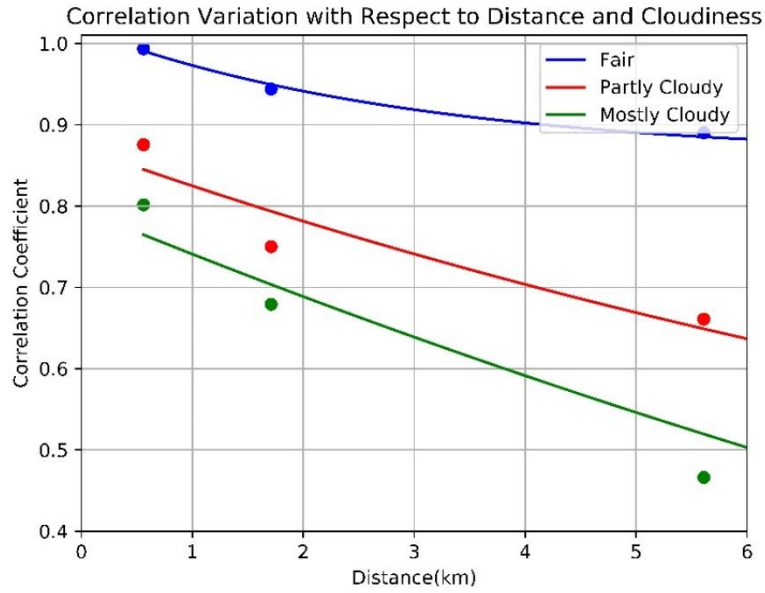
Figure 3-3. Correlation Variation with Respect to Distance and Cloudiness up to 6 km

5 km can be considered as good distance because BTM PV generations in Ankara which is a quite big city can be predicted with just 10 representative sites as illustrated in Fig. 3-4.

Figure 3-4. Example Sub-regions of Ankara

Step-2. Weather Condition Identification

The weather condition identification aims to classify the cloudiness of the sky, based on the recorded power generation data. Although cloudiness level is published online by many different sources, it in general corresponds to a large area for a long duration (hours) and may not reflect the actual condition at the considered region. More accurate information about cloudiness level is required to obtain more accurate predictions.

The daily generation curve of a PV system varies according to effective solar irradiation reaching the surface of the solar panels. It has a continuous cosine-like shape on a sunny day, while it is distorted on cloudy days. The similarity between the solar power generation pattern and cosine function is visualized in Fig. 3-5.
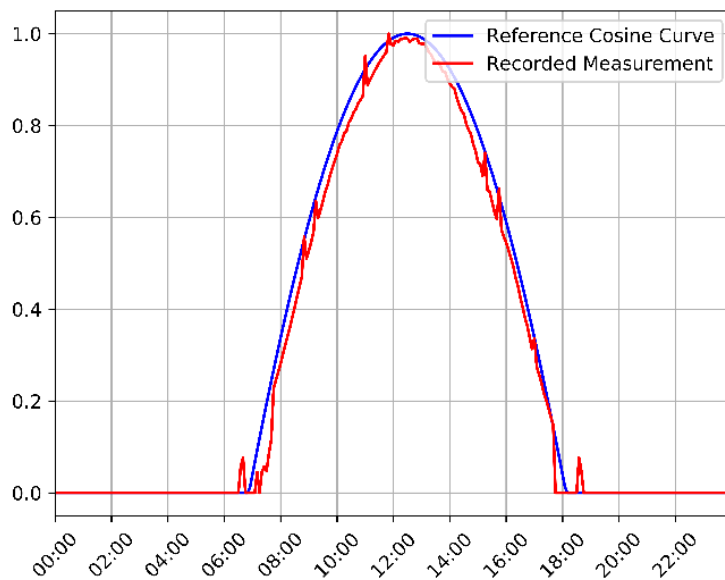
Figure 3-5. Normalized Generation vs. Reference Cosine Function

In order to categorize days, this similarity is utilized, such that a cosine curve which is adjusted according to sunshine duration and expected rated power generation corresponding to the considered day is compared to the gathered measurements. The comparison is performed with values corresponding to the most up-to-date one hour assuming the measurements are collected once in every five minutes, since cloudiness

level may change during a day. The deviation of the measured values from the cosine curve is used as the measure of the similarity, where:

$$\sigma_t = \sqrt{\frac{\|\bar{x}[t - N + 1:t] - x[t - N + 1:t]\|}{N}} \qquad (3.2)$$

where:

σ_t is the deviation amount between reference cosine curve and the measurements at time instant $'t'$,

$\bar{x}[t - N + 1:t]$ is the reference cosine curve,

$x[t - N + 1:t]$ is the vector of recorded measurements,

N is the number samples corresponding to one hour.

As mentioned in the previous sub-section, days are categorized into three groups based on the cloudiness. Therefore, two threshold values, such as σ_1 and σ_2 should be chosen. Those threshold values can be determined heuristically by examining the obtained σ_t values and the observed cloudiness level. For instance, in this study, threshold values are determined by comparing cosine-like function and existing measurements taken before and cloud cover index. These values will probably change depending on the location of PV systems among all over the world. The flow chart of the cloudiness level detection is presented in Fig. 3-6.
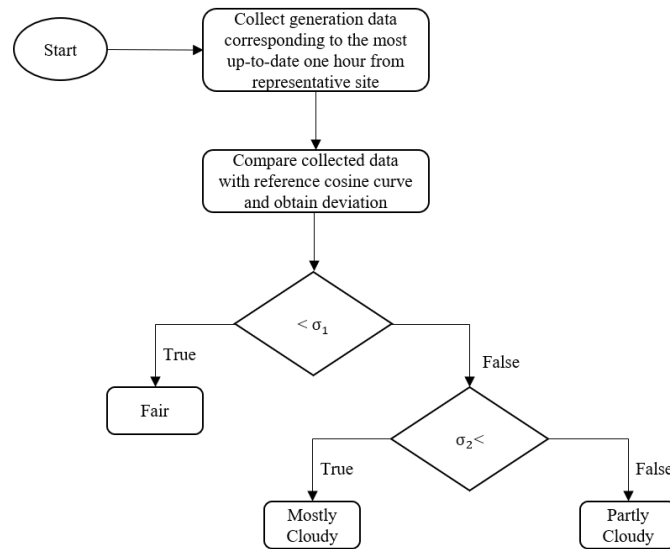
Figure 3-6. Flow Chart for the Cloudiness Level Detection

Step-3. Prediction of Behind-the-Meter PV Generation

The power generation of a PV system can be predicted based on another PV system power generation, which is the representative site, using conditional expectation. To define the conditional expectation relation, firstly the probabilistic distribution should be investigated. It is known that the probability distribution of the solar power generation is Gaussian. Having the three cloudiness level categories, the mean and variance values will differ for each category.

If two variables have normal distribution, and they have a normal distribution when both are added together, it is said that those variables are in a bivariate normal. Fig. 3-7 shows the bivariate normal distribution of the solar power generation deviation from expected generations recorded on cloudy days, and recorded at two location, which are 1.2 km apart.

41
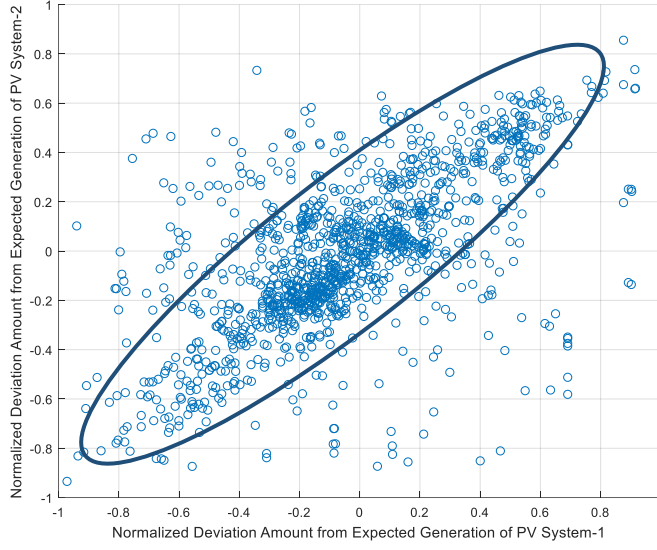
Figure 3-7. Bivariate Normal Distribution

Having a bivariate normal distribution, the conditional expectation between the reference site and other PV systems can be represented as follows.

$$E(Y_d^w|X^w) = E(Y_d^w) + \rho_{X^w Y_d^w}\sigma_{Y_d^w}\frac{X^w - E(X^w)}{\sigma_{X^w}} \tag{3.3}$$

where,

$E(X^w)$ is the expectation (mean) of X^w

$E(Y^w)$ is the expectation of Y_d^w,

$E(Y_d^w|X^w)$ is the conditional expectation of Y_d^w given X^w,

$\rho_{X^w Y_d^w}$, σ_{X^w} and $\sigma_{Y_d^w}$ are determined using the collected data at *Step-1*. Although power generation amounts of two PV systems are dependent on the cloudiness level of the sky, they are independent of each other so $(Y_d^w) = KE(X^w)$, and $\sigma_{Y_d^w} = K\sigma_{X^w}$, and hence (3) can be reformulated as follows.

$$E(Y_d^w|X^w) = K\rho_{X^w Y_d^w}X^w + \left(1 - \rho_{X^w Y_d^w}\right)KE(X^w) \tag{3.4}$$

42

where,

K is the ratio of the rated power of the unmonitored PV system to that of the representative site.

3.2. Actual Load Demand Prediction

Prediction of actual load demand is conducted based on the measurement taken from distribution substation which indicates the power drawn from the transmission system. This power does not represent the actual power consumed within the distribution system because some amount of load is supplied by distributed PV systems within distribution system. Hence, measurements can be considered as net load demand for that distribution system.

Then, the net load from the grid P_{net} for any given time t for distribution systems with high PV penetration can be expressed as,

$$P_{net}(t) = P_T(t) - P_{pv}(t) \qquad (3.5)$$

where,

$P_T(t)$ is the total or actual load,

$P_{pv}(t)$ is the load demand met by solar power generated by PV systems,

Thus, if the PV generations can be added to the net load, then a more accurate actual load demand prediction can be achieved. However, a high percentage of the PV systems in distribution system are not monitored due to additional cost for sensors, data logging equipment and communication.

The basic idea of the proposed method is thus first predicting total power generation of unmonitored PV systems by using proposed method, and second predicting the actual load demand by adding PV generations to the net load. Since load demand is periodic, it is possible to use well-developed Kalman filter algorithm to determine the

43

actual load in each time step considering that measurements have uncertainties due to measurement and process error.

For a system with high PV penetration, mainly in the form of small-scale roof-top PV, the equations for Kalman filter can be constructed as follows,

$$P_{L,k} = P_{L,k-1,k-1} + A_{L,k-1} + w_{k-1}$$

(3.6)

$$P_{inj,k} = P_{L,k} - P_{PV,k} + v_k$$

(3.7)

where,

$P_{L,k}$ is the actual demand at time instant k,

$P_{inj,k}$ is the net load measurement at the substation at time instant k,

$A_{L,k-1}$ is the expected demand change at time instant $k-1$,

$P_{PV,k}$ is the total PV generation prediction within distribution network at time instant k,

w_{k-1} is the process noise at time instant $k-1$,

v_k is the measurement noise at time instant k.

After starting with initial assumptions, actual loads for each time step k, can be predicted by Kalman filter's prediction followed by correction process.

3.3. Chapter Summary and Conclusions

In this chapter, BTM PV generation prediction and actual load demand prediction methods were proposed. The method proposed for BTM PV generation prediction has three main steps. In the first step, solar radiation data are collected from the specified sub-regions to model the relation between the solar irradiation of various points and the representative site. This step is a one-time job conducted before running the proposed prediction and does not need to be reperformed when new PV systems are

installed. Thus, the method can easily adopt the future growth of capacity of BTM PV systems. In the second step, cloudiness level detection is applied in order to categorize days. This is because correlation versus distance curves are obtained for each type of days namely, fair, partly cloudy, mostly cloudy separately in the first step by using same cloudiness level detection algorithm. Since the correlation is also affected by cloudiness amount as well as distance between representative sites and any point in considered area, cloudiness level of day should be considered for more accurate prediction. In the last step, generations of BTM PV systems within the specified sub-regions are predicted by using conditional expectation.

Once the method starts prediction, firstly cloudiness characterization is performed, followed by the computation of conditional expectation of the generation of BTM PV systems by using correlation coefficient which is obtained in first stage.

The method proposed for actual load demand prediction is based on well-known Kalman filtering algorithm. The contribution here is taking PV generations which is not actually known or monitored and has direct impact on load demand into account unlike traditional methods.

CHAPTER 4

TESTS AND EVALUATION OF THE PROPOSED METHOD

This chapter presents the conducted tests and numerical results to validate the proposed method. Three different tests are done in order to validate three main parts of the proposed method, namely cloudiness level detection, total PV generation prediction and actual load demand prediction. Results of these tests are illustrated under related subsections.

4.1. Weather Condition Identification

This section presents the result of weather condition identification algorithm which is explained in the previous chapter. Fig. 4-1(a) shows the determined cloudiness levels corresponding to each hour of a single day. The solar power generation recorded on this day can be seen in Fig. 4-1(b). The deviation in the morning hours are higher, since the mismatch between the used reference cosine function and the realized power generation is higher. The cosine function is used for the sake of simplicity. One may use a fitted generation curve as the reference. The σ_1 and σ_2 are determined by examining the data. Note that, those values may change based on the geographical location of the considered region.
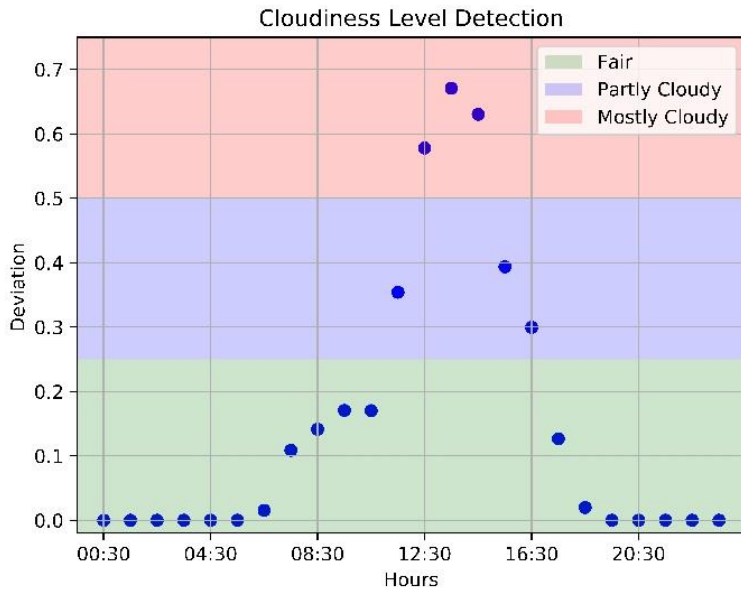
(a) Cloudiness Level Classification
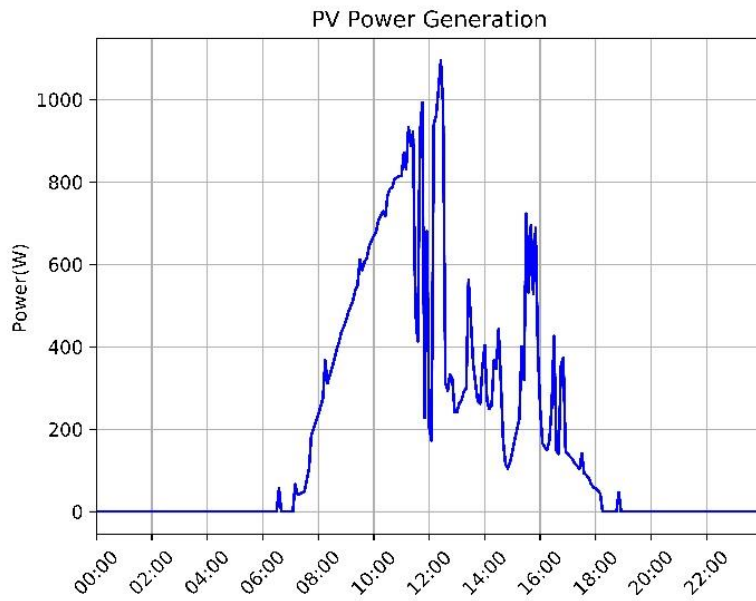
(b) PV Generation

Figure 4-1. Power Generation on the Cloudiness Level Classified Day

48

It can be obviously seen that the algorithm is for predicting cloudiness level if the thresholds σ_1 and σ_2 are chosen appropriate.

4.2. Total PV Generation Prediction

This section presents tests and evaluation of the proposed method for predicting total solar power generation individually. In this work, the solar radiation data is collected in the city of Ankara, Turkey, using pyranometers. The representative site is located at the Department of Electrical and Electronics Engineering of the Middle East Technical University (METU) shown by red map marker on Fig. 4-2 and solar irradiation is continuously recorded with pyranometer as can be seen in Fig. 4-3. The other data collection points which simulate behind-the-meter PV panels are shown by blue map markers on Fig. 4-2 and solar irradiation is recorded with mobile pyranometer as shown in Fig. 4-4. Besides the irradiation data, solar power generation data corresponding to the 50 kWp PV system located at METU are also utilized for the statistical analysis of the solar power generation with respect to weather conditions. All power generation data are recorded with 5-minute intervals for each day from 01.01.2013 to 31.12.2016.
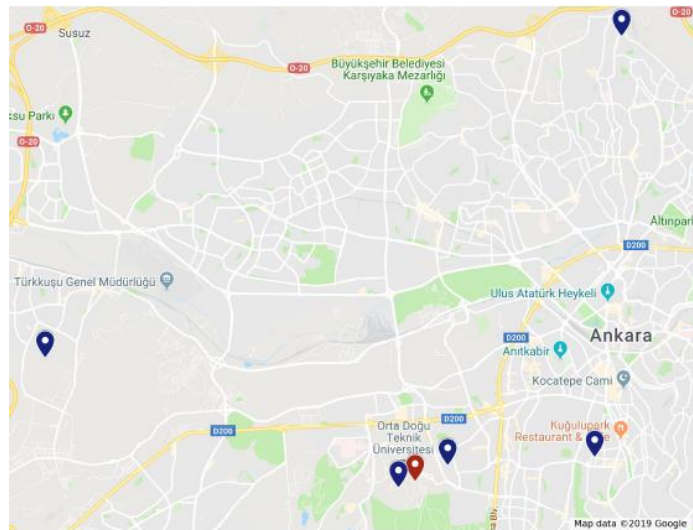
Figure 4-2. Data Collection Points

Figure 4-3. Pyranometer Used in Representative Site

Figure 4-4. Pyranometer Used in Data Collection Points

Fig. 4-5 shows the relation between the irradiation data and solar power generation. Considering Fig. 4-5, it can be concluded that the solar power generation is highly correlated to solar irradiation, and hence the relation among the solar irradiation data of different locations can be applied to solar power generation amounts as well. In other words, one can use both power generation and solar irradiation data to employ the proposed method.
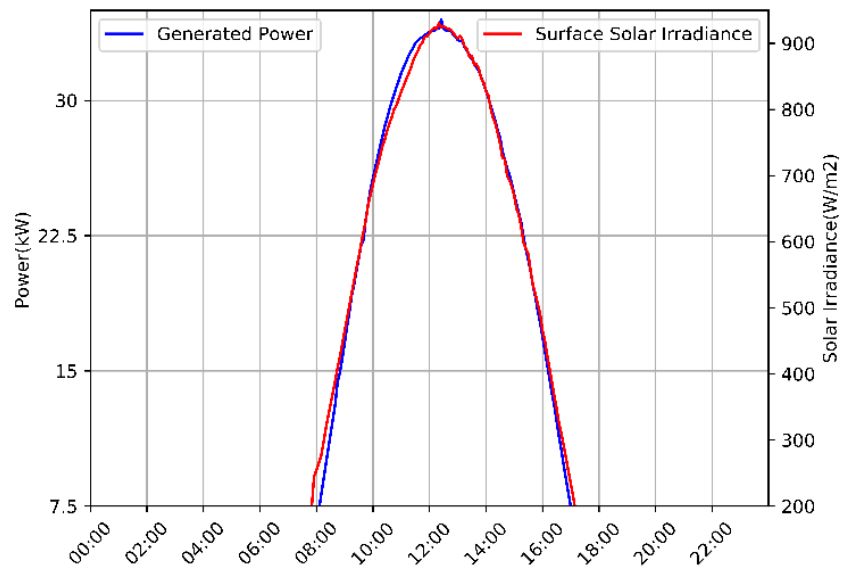
(a) Power Generation Data and Solar Irradiation Data – Fair Day
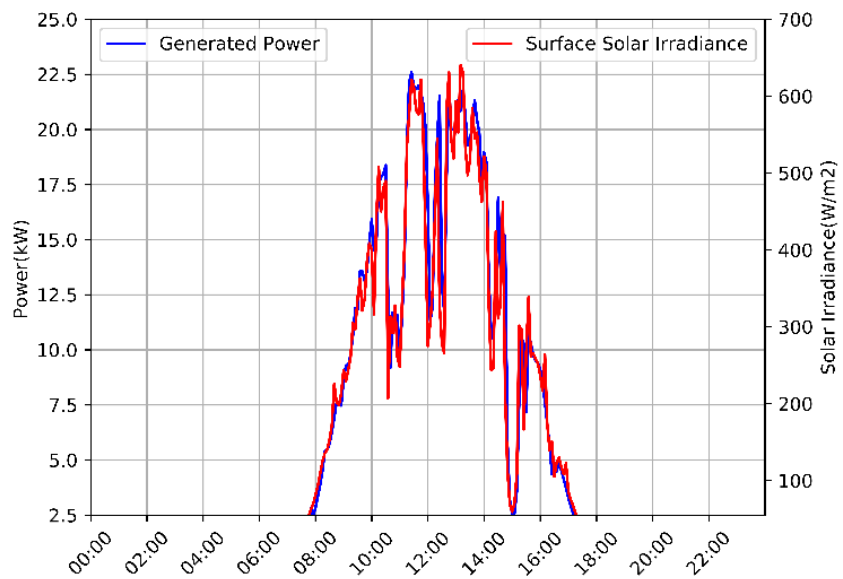
(b) Power Generation Data and Solar Irradiation Data – Cloudy Day

Figure 4-5. Generation and Irradiation Data Recorded Under Different Weather Conditions

51

As mentioned in Chapter 2, the collected data was used to form the correlation regression curves with respect to distance to the representative site for all three cloudiness level categories. The obtained curves are shown in Fig. 3-3. As seen in Fig. 3-3, as the distance increases, fitting the correlation to a function becomes more cumbersome, therefore the distance between the representative site and the other PV systems should be limited. For this experiment, it seems the method is capable of being good predictions in sub-region with 5 km radius. Note that, the correlation values significantly differ for different cloudiness level. Therefore, to obtain a more accurate predict, it is essential to form specific correlation curves for each weather condition.

Once the correlation values are determined, the proposed method can be run with real time data. In the real time operation, the first step is the classification of each hour based on cloudiness level with proposed algorithm tested in previous sub-section, as proper correlation values should be utilized.

The power production of PV plant that is not monitored can be predicted based on (3.4). The results of the proposed method are compared to the measured realization and presented in Fig. 4-6. The mismatch between the prediction and the realization is quantified using the root mean square error (RMSE), which is defined below. The RMSE values for different cases are presented in Table 1.

$$RMSE = \sqrt{mean((P_{real} - P_{estimated})^2)} \qquad (4.1)$$

where,

P_{real} is the vector of realized power generation values,

$P_{prediction}$ is the vector of predicted power generation values.
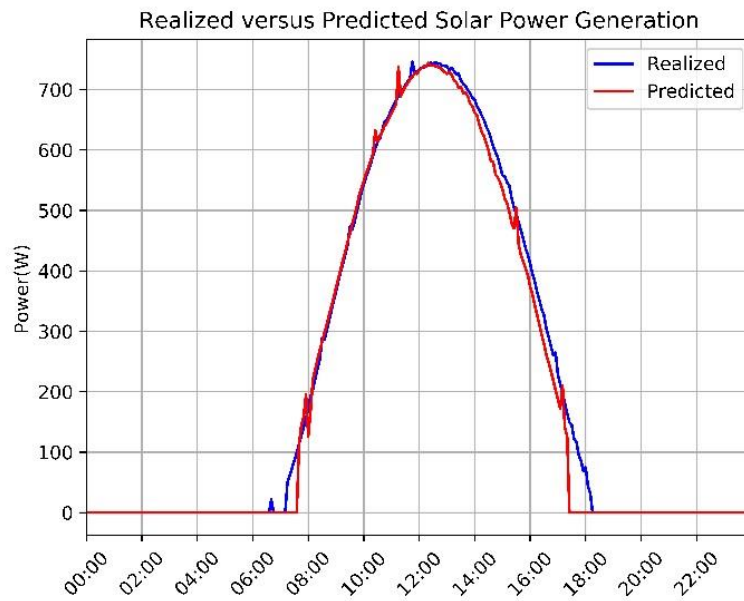
(a) Fair day, Distance Between the Representative Site and the Predicted PV Generation is 0.6 km
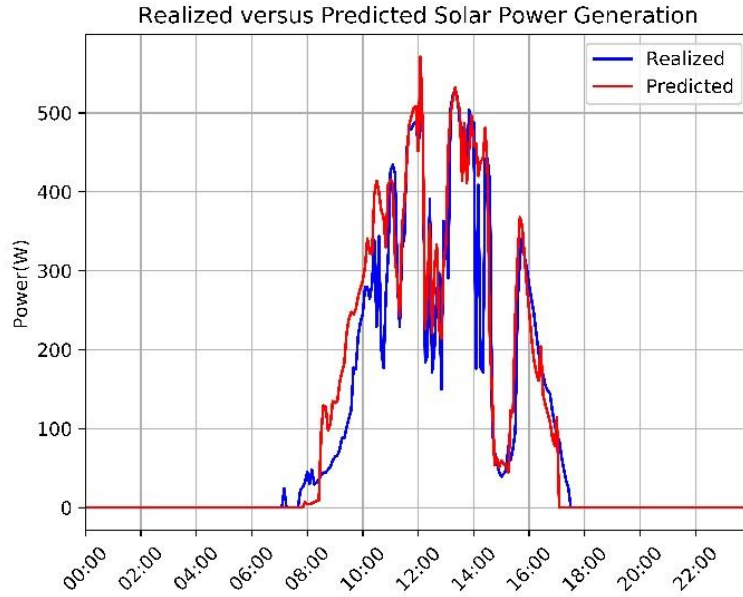
(b) Cloudy day, Distance Between the Representative Site and the Predicted PV Generation is 1.75 km
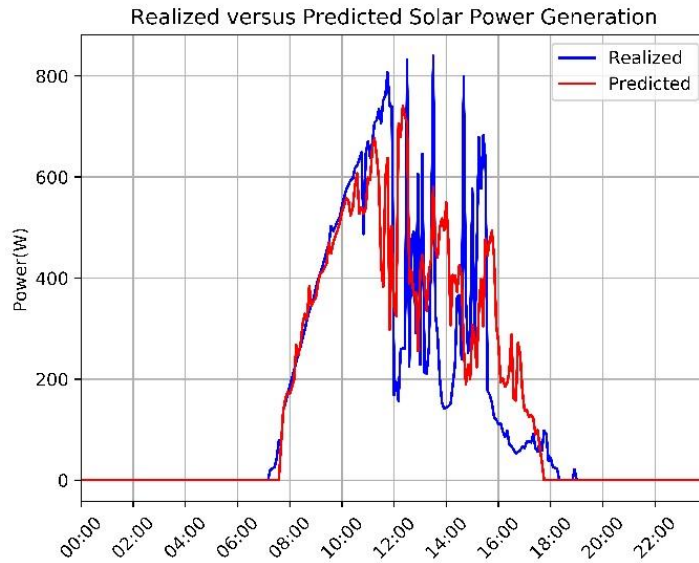
(c) Cloudy day, Distance Between the Representative Site and the Predicted PV Generation is 12.5 km

Figure 4-6. Predicted vs. Measured Solar Power Generation for Different Distances and Types of Days

Table 4-1. *RMSE Values*

	d=0.6km	d=5.6km	d=12km
Fair	4%	12.8%	14.9%
Partly Cloudy	10.2%	18.2 %	24.9%
Mostly Cloudy	13.9%	-	27.4%

4.3. Actual Load Demand Prediction

This section presents test and evaluation of the proposed method for predicting actual load based on prediction of total PV generation obtained in previous step. The algorithm is developed on MATLAB platform to implement power flow analysis and Kalman filtering. In this work, IEEE 33 bus radial distribution system which can be seen in Appendix A is modified to use as test case. Eight PV systems are connected to different load points in the system. Four of them are stated as representative PV sites

which are being monitored continuously, and others are not monitored, and their generations are predicted. Since total PV generation was predicted at 5-minute intervals, injected power values at distribution substation point are needed to be specified at each 5-minute. Since system data has only instantaneous load demand for each bus, it is extended to have 5-minutes intervals such that each bus has daily load profile in 5-minute resolution and system data is the peak value of a day. The structure of typical radial distribution network can be represented as in Fig. 4-7.
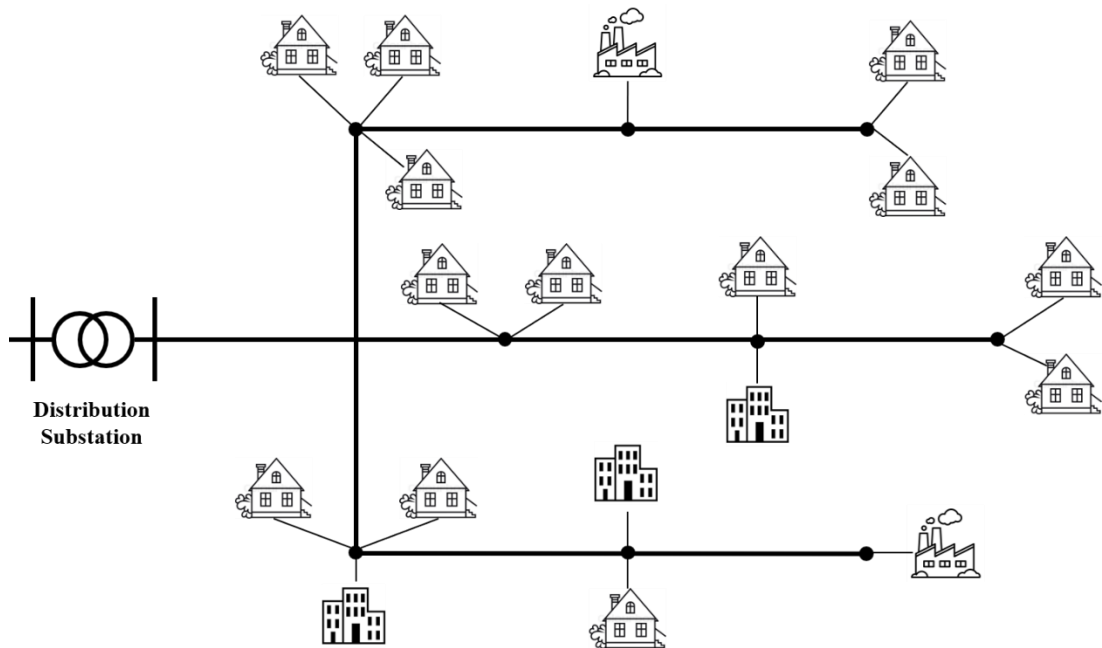
Figure 4-7. Example of Radial Distribution Network Supplying Different Types of Loads

In order to get more realistic results daily load profile for each bus is created according to different types of load which can be in distribution network. Typical daily load profiles for different types of load can be seen in Fig. 4-8.
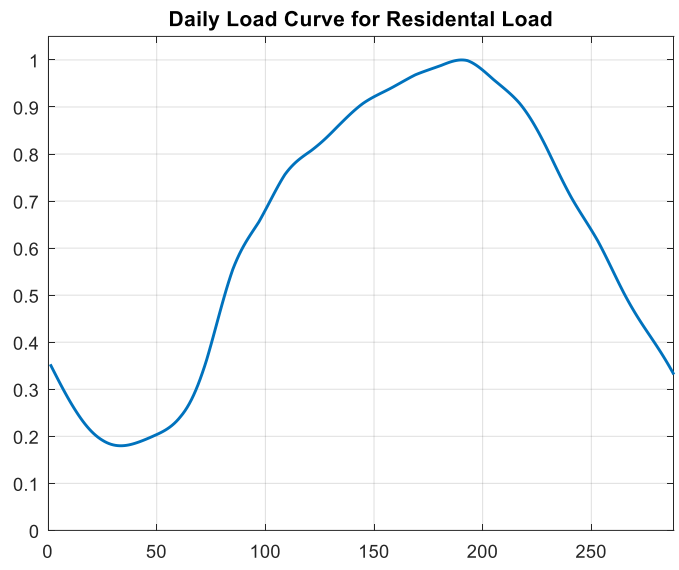
(a) Daily Load Curve for Residential Load
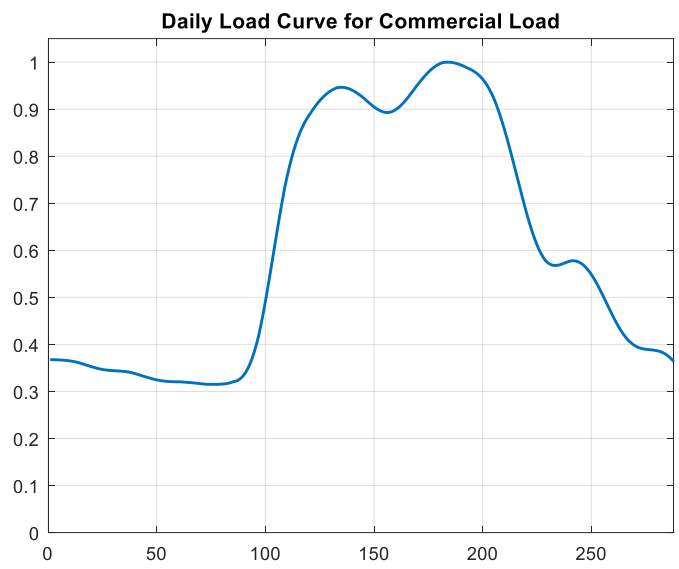
(b) Daily Load Curve for Commercial Load

Daily Load Curve for Industrial Load
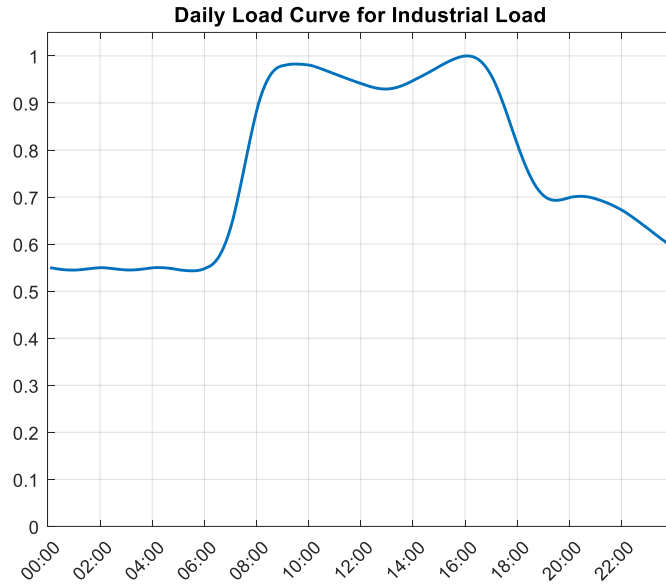
(c) Daily Load Curve for Industrial Load

Figure 4-8. Daily Load Curves for Different Types of Load

The algorithm is developed on MATLAB platform using MATPOWER tool to perform the load flow analysis to obtain injected powers at substation point. MATPOWER is an open-source optimization and simulation tool implemented in MATLAB for power grid research. It is capable of providing power flow and optimal power flow solution. It has several test cases both transmission and distribution system for which power flow problem can be solved with command in just one-line [45]. Power flow is solved for a single day in order to obtain measurements at the HV/MV transformer substation at 5-minute interval. Example output of power flow calculations by MATPOWER can be seen in Appendix B. After perform load flow analysis and obtain measurements at 5-minute interval, Kalman filter algorithm is implemented in MATLAB as stated in Table 4-2.

Table 4-2. Implemented Kalman Filter Algorithm

Prediction	Update
$P_{L,k}{}^- = P_{L,k-1} + A_{L,k-1}$ $P_k{}^- = P_{k-1} + Q_{k-1}$	$K_k = \dfrac{P_k{}^-}{P_k{}^- + R}$ $P_{L,k} = P_{L,k}{}^- + K_k \left(P_{inj,k} + P_{PV,k} - P_{L,k}{}^- \right)$ $P_k = (1 - K_k)\, P_k{}^-$

The implemented Kalman filtering is executed over 288-time steps, and the predicted and true actual load are provided in Fig. 4-9.
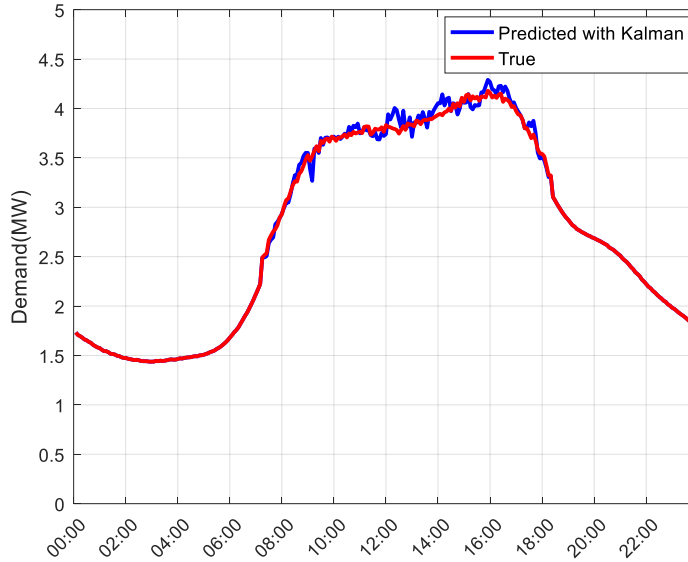
Figure 4-9. Predicted by Kalman Filtering and True Actual Load

If the proposed method for predicting total PV generation is not used and unmonitored PV systems' generations are considered to be equal to monitored PV, the daily load curve would be assumed as in Fig. 4-10.

58
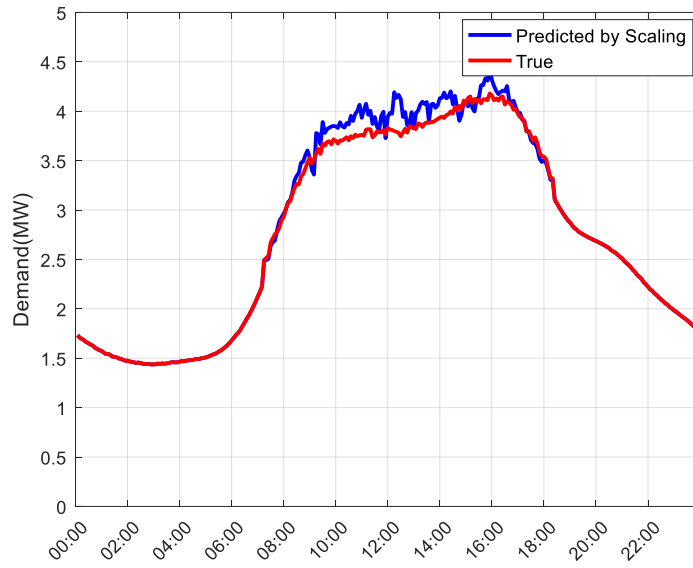
Figure 4-10. Predicted by Scaling and True Actual Load

If only monitored PV systems are considered and added on measurement at HV/MV transformer substation without considering the unmonitored PV systems, the daily load curve would be assumed as in Fig. 4-11.
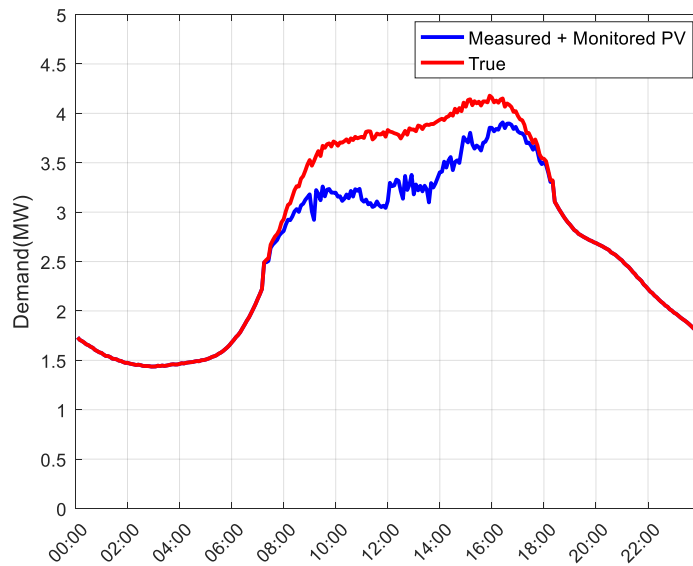
Figure 4-11. Measured Plus Monitored PV Generation and True Load

If monitored PV generations are also not considered and only measurement at HV/MV transformer substation is considered as load which conventional load demand estimation methods do, then the daily load curve would be assumed as in Fig. 4-12.
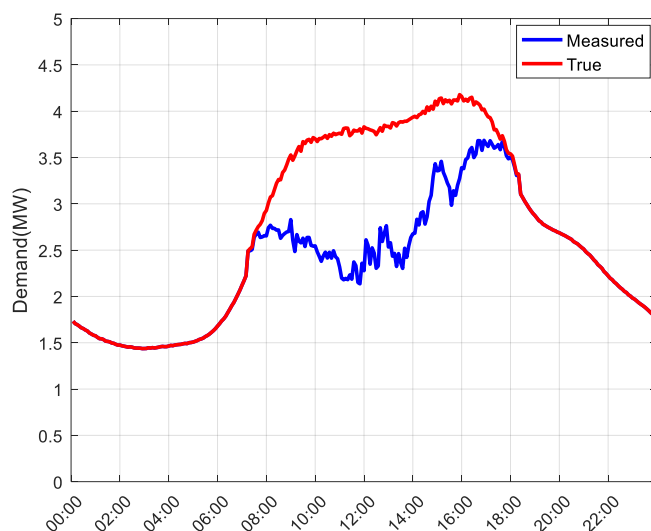
Figure 4-12. Measured and True Load

Additional tests are conducted in order to observe performance of proposed method if the efficiencies of unmonitored PV's decrease. As expected, error between predicted actual load demand and real actual load demand increases, however Kalman filtering tries to reduce uncertainties by providing smoothing and gives better results than directly adding net load demand and total PV generation prediction.
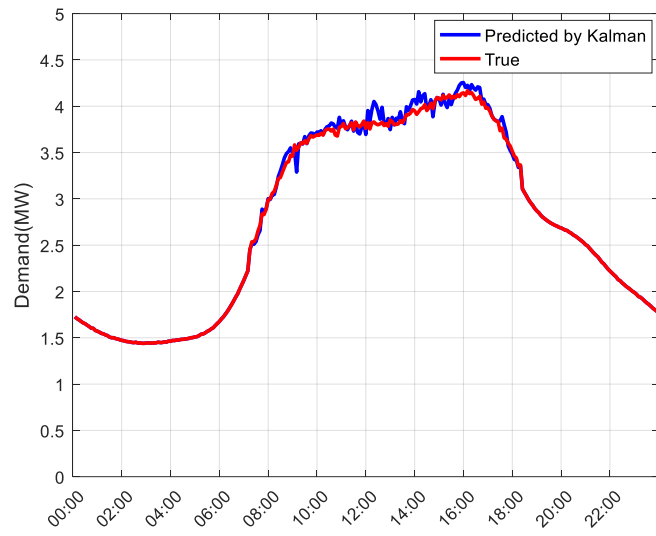
(a) When One PV's Efficiency Drops to 90%
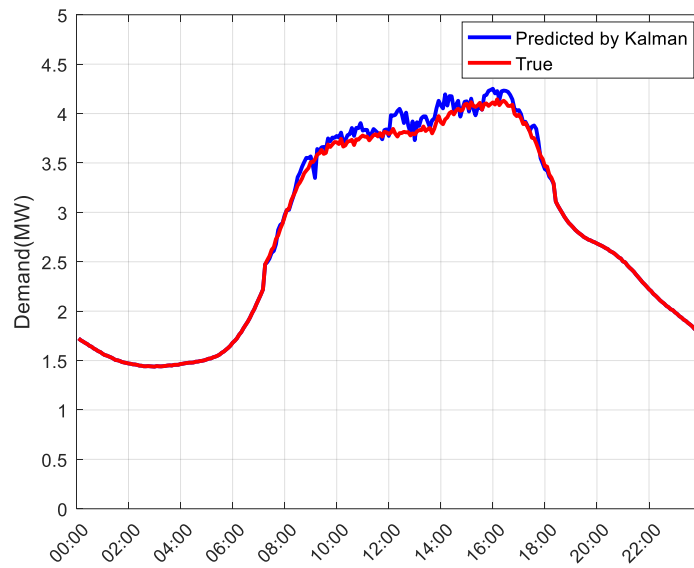
(b) When All Four PV's Efficiencies Drop to 90%

61
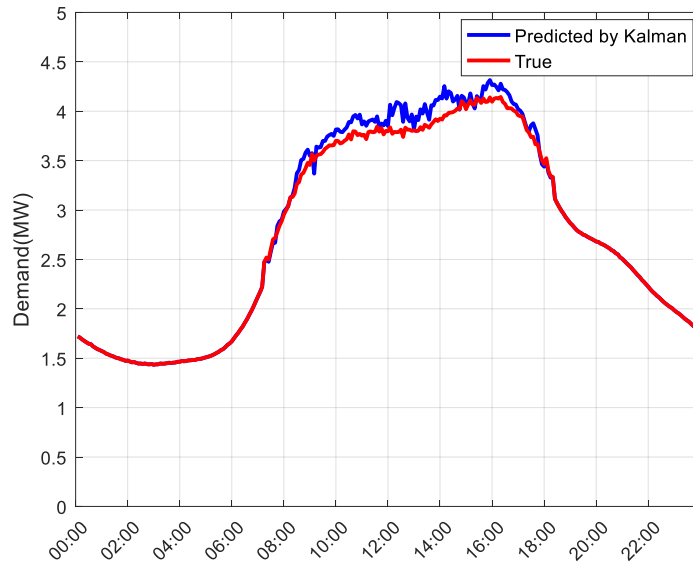
(c) When All Four PV's Efficiencies Drop to 80%

Figure 4-13. Predicted by Kalman Filtering and True Actual Load when PV Efficiency Drops

4.4. Chapter Summary and Conclusions

In this chapter, tests and evaluations for proposed methods was conducted. The results showed that the proposed method can predict the generation of BTM PV systems with a good accuracy up to a certain distance with inversely proportional to the cloudiness level. The accuracy of the proposed method can be improved by increasing number of the representative sites, and hence decreasing the size of the region of interest and collecting more data before prediction process. For the actual load demand prediction method, it is superior to traditional methods accuracy mostly depends on the accuracy of BTM generation prediction method. When the penetration of BTM PV systems is quite low, actual load demand can be found by simply adding predicted BTM PV generation to the net load measurements. However, when the penetration of BTM PV systems increases, Kalman filtering gives better results by considering uncertainties in all measurements.

CHAPTER 5

CONCLUSION AND FUTURE WORK

Load demand forecasting is extremely important for power system operators in electricity generation, transmission, distribution and markets. Accurate models for load demand forecasting are essential to the operation and planning of a power system. However, because of the increasing PV penetration at the distribution system, mainly the small size of the roof-top PV systems, the existing forecast model's accuracy drops. Because all of those methods require proper set of data however, as the number of BTM PV systems increases, the collected data by system operators become related to net demand, rather than the actual power demand considering that the distribution systems are monitored only at the substations between the transmission and distribution networks. As a result of this, determining the actual power demand of the customers become problematic.

The main motivation of this thesis is to develop a method for predicting actual load demand with better accuracies. Although the main focus of the thesis was the predicting actual load demand, a method for predicting BTM PV generation is also developed. The proposed method predicts actual load demand by assuming:

- the rated power and location of every single PV system in considered area is known.
- Any obstacle except moving clouds does not block sunlight over the PV systems during the day.
- Any factor affecting the efficiency of PV systems affects all PV systems in considered area in the same way.

The contribution of the proposed work can be listed as follows:

- The proposed method provides actual load demand prediction.

- The proposed method does not require continuous measurement of every single PV system at the considered area, rather characterizes the generation profiles of PV systems at different locations under various weather conditions based on prior measurements.

- Communication burden of the proposed method is low.

- Computational complexity of the proposed method is low.

- The proposed method provides automatic weather condition classification based on the measurement to prevent continuous data acquisition from meteorological center and to improve accuracy of available weather forecasts.

Future work can focus on demonstrating the algorithm on real distribution system with real data. In addition, the algorithm can be demonstrated on larger cities with larger data set. Finally, further analysis of the algorithm's sensitivity to additional system changes can be investigated.

REFERENCES

[1] Global Market Outlook for Photovoltaics 2019-2023 [Online]. Available: http://www.solarpowereurope.org/wp-content/uploads/2019/05/SolarPower-Europe-Global-Market-Outlook-2019-2023.pdf, accessed Mar. 1, 2019.

[2] Sobri S, Koohi-Kamali S, Rahim, Solar photovoltaic generation forecasting methods: a review. Energy Convers. Manag. (2018) 459-497.

[3] Das UK, Tey KS, Seyedmahmoudian M, Mekhilef S, Idris MYI, Van Deventer W, et al. Forecasting of photovoltaic power generation and model optimization: a review. Renew Sustain Energy Rev 2018; pp. 81:912–28.

[4] Antonanzas, J., Osorio, N., Escobar, R., Urraca, R., Martinez-de-Pison, F.J., Antonanzas-Torres, F. Review of photovoltaic power forecasting, Sol. Energy 2016, 15, 78-111.

[5] Voyant, C.; Notton, G.; Kalogirou, S.; Nivet, M.L.; Paoli, C.; Motte, F.; Fouilloy, A. Machine learning methods for solar radiation forecasting: A review. Renew. Energy 2017, 1, 569–582.

[6] H. Shaker, H. Zareipour, and D. Wood, "A data-driven approach for estimating the power generation of invisible solar sites," IEEE Trans. Smart Grid, vol. 7, no. 5, pp. 2466–2476, Sep. 2016.

[7] H. Shaker, H. Zareipour, and D. Wood, "Estimating power generation of invisible solar sites using publicly available data," IEEE Trans. Smart Grid, vol. 7, no. 5, pp. 2456–2465, Sep. 2016.

[8] Papalexopoulos A.D., Hesterberg T.C.: 'A regression-based approach to short-term system load forecasting', IEEE Trans. Power Syst., 1990, 5, (4), pp. 1535–1547

[9] Bianco, V., Manca, O., Nardini, S., Electricity consumption forecasting in Italy using linear regression models. Energy 2009;34:1413-21. 60

[10] Hong, T., Wilson, J., Xie, J.: 'Long term probabilistic load forecasting and normalization with hourly information', IEEE Trans. Smart Grid, 2014, 5, (1), pp. 456–462.

[11] Amral, N.; Ozveren, C.S.; King, D. Short term load forecasting using Multiple Linear Regression. In Proceedings of the 2007 42nd International Universities Power Engineering Conference, Brighton, UK, 4–6 September 2007; pp. 1192–1198

[12] Kim, J., Cho, S., Ko, K., & Rao, R.R. (2018). Short-term Electric Load Prediction Using Multiple Linear Regression Method. 2018 IEEE International Conference on Communications, Control, and Computing Technologies for Smart Grids (SmartGridComm), 1-6.

[13] S. J. Huang and K. R. Shih, "Short-term load forecasting via ARMA model identification including non-Gaussian process considerations," IEEE Trans. Power Syst., vol. 18, pp. 673-679, Feb.2003.

[14] L.C.M de Andrade, and I.N. da Silva, "Very short-term load forecasting based on ARIMA model and intelligent systems", 15th International Conference on Intelligent System Applications to Power Systems (ISAP '09), pp. 1-6, 8-12 Nov 2009.

[15] Christiaanse, W.R.: 'Short-term load forecasting using general exponential smoothing', IEEE Trans. Power Appar. Syst., 1971, 90, (2), pp. 900–911

[16] P. Ji, D. Xiong, P. Wang, and J. Chen, "A study on exponential smoothing model for load forecasting," in Asia-Pacific Power and Energy Engineering Conference, APPEEC, 2012.

[17] Al-Hamadi HM, Soliman SA. Short-term electric load forecasting based on Kalmanfiltering algorithm with moving window weather and load model. Electr Power SystRes 2004;68:47–59.

[18] D. C. Park et al., "Electric load forecasting using an artificial neural network," IEEE Trans. Power Syst., vol. 6, pp. 442–449, May 1991.

[19] H. S. Hippert, C. E. Pedreira, and R. C. Souza. Neural networks for short-term load forecasting: A review and evaluation. IEEE Transactions on power systems, 16(1):44–55, 2001.

[20] Ding, N., Benoit, C., Foggia, G., et al.: 'Neural network-based model design for short-term load forecast in distribution systems', IEEE Trans. Power Syst., 2016, 31, (1), pp. 72–81.

[21] Chen, B.J., Chang, M.W., Lin, C.J.: 'Load forecasting using support vector machines: a study on eunite competition 2001', IEEE Trans. Power Syst., 2004, 19, pp. 1821–1830. 61

[22] S.H. Ling, F.H.F. Leung, H.K. Lam, Y.S. Lee and P.K.S. Tam, "A novel GA-based neural network for short-term load forecasting," IEEE Trans. Industrial Electronics., Vol.50, No.4, pp.793-799, Aug 2003.

[23] A. Jain, B. Satish, " Clustering based Short Term Load Forecasting using Support Vector Machines", IEEE Bucharest Power Tech Conference, 2009.

[24] E. E. Elattar, J. Goulermas, and Q. H. Wu, ''Electric load forecasting based on locally weighted support vector regression,'' IEEE Trans. Syst., Man, Cybern. C, Appl. Rev., vol. 40, no. 4, pp. 438–447, Jul. 2010.

[25] A. G. Bakirtzis, J. B. Theocharis, S. J. Kiartzis and K. J. A. Satsios, "Short term load forecasting using fuzzy neural networks," IEEE Transactions on Power Systems, pp. 1518-1524, Aug 1995.

[26] Kaur A, Nonnenmacher L, Coimbra CFM. Net load forecasting for high renewable energy penetration grids. Energy 2016;114:1073–84.

[27] Yu Liu, Zhi Li, Kai Bai, Zhaoguang Zhang, Xining Lu, Xiaomeng Zhang, "Short-term power-forecasting method of distributed PV power system for consideration of its effects on load forecasting," The Journal of Engineering, vol. 2017, no.13, pp. 865 - 869, 2017.

[28] Y. Wang, N. Zhang, Q. Chen, D. S. Kirschen, P. Li, and Q. Xia, "Data-driven probabilistic net load forecasting with high penetration of behind-the-meter PV," IEEE Trans. Power Syst., vol. 33, no. 3, pp. 3255–3264, May 2018.

[29] Cook, G., Billman, L., Adcock, R., Solar Technical Information Program (U.S.), United States., & National Renewable Energy Laboratory (U.S.). (1995). Photovoltaic fundamentals. Washington, DC: National Renewable Energy Laboratory.

[30] Mertens, K. (2014). Photovoltaics: Fundamentals, technology and practice.

[31] Ekins-Daukes, N., Merlinde, N. (2019). Brighten the dark skies. Nature Energy, 4(8), 633–634. doi: https://doi.org/10.1038/s41560-019-0440-0

[32] Global Solar Atlas, 2017. The World Bank Group. https://globalsolaratlas.info.

[33] Wikipedia: The free encyclopedia. (2004, July 22). FL: Wikimedia Foundation, Inc. Retrieved July 10, 2019, from https://en.wikipedia.org/wiki/File:Solar_cell.png

[34] Introduction to Photovoltaic Systems, Renewable Energy, the Infinite Power of Texas, SECO Fact Sheet No. 11.

[35] A. B. Oskouei, M. R. Banaei, and M. Sabahi, "Hybrid PV/wind system with quinary asymmetric inverter without increasing DC-link number," Ain Shams Engineering Journal, vol. 7, pp. 579-592, 2016.

[36] J. Sreedevi, N. Ashwin, "A study on grid connected PV system", 2016 National Power Systems Conference (NPSC, 2016).

[37] Tobnaghi, D. (2016). 'A Review on Impacts of Grid-Connected PV System on Distribution Networks'. World Academy of Science, Engineering and Technology, 62 Open Science Index 109, International Journal of Electrical and Computer Engineering, 10(1), 137 - 152.

[38] S. J. Lewis, "Analysis and management of the impacts of a high penetration of photovoltaic systems in an electricity distribution network", *Proc. IEEE PES Innovative Smart Grid Technol.*, pp. 1-7, 2011.

[39] A. Patil, R. Girgaonkar, S.M. Musunuri, "Impact of Increasing Photovoltaic Penetration on Distribution Grid — Voltage Rise Case Study", IEEE International Conference on Advances in Green Energy, vol. 3, Dec. 2014.

[40] Wikipedia: The free encyclopedia. (2004, July 22). FL: Wikimedia Foundation, Inc. Retrieved July 10, 2019, from http://en.wikipedia.org/wiki/File:Normal_Distribution_PDF.svg

[41] Wikipedia: The free encyclopedia. (2004, July 22). FL: Wikimedia Foundation, Inc. Retrieved July 10, 2019, from http://en.wikipedia.org/wiki/File:Standard_deviation_diagram.svg

[42] Wikipedia: The free encyclopedia. (2004, July 22). FL: Wikimedia Foundation, Inc. Retrieved July 10, 2019, from http://en.wikipedia.org/wiki/File:MultivariateNormal.png

[43] M. Lave, J. Kleissl, and J. S. Stein, "A wavelet-based variability model (WVM) for solar PV power plants," IEEE Trans. Sustain. Energy, vol. 4, no. 2, pp. 501–509, Apr. 2013.

[44] M. B. P. de Camargoa and K. G. Hubbard, "Spatial and temporal variability of daily weather variables in sub-humid and semi-arid areas of the United States high plains," Agric. Forest Meteorol., vol. 93, no. 2, pp. 141–148, Aug. 1998.

[45] R. D. Zimmerman, C. E. Murillo-Sanchez, Matpower 7.0 User's Manual, [online] Available: https://matpower.org/docs/manual.pdf

APPENDIX A

33 BUS RADIAL DISTRIBUTION SYSTEM
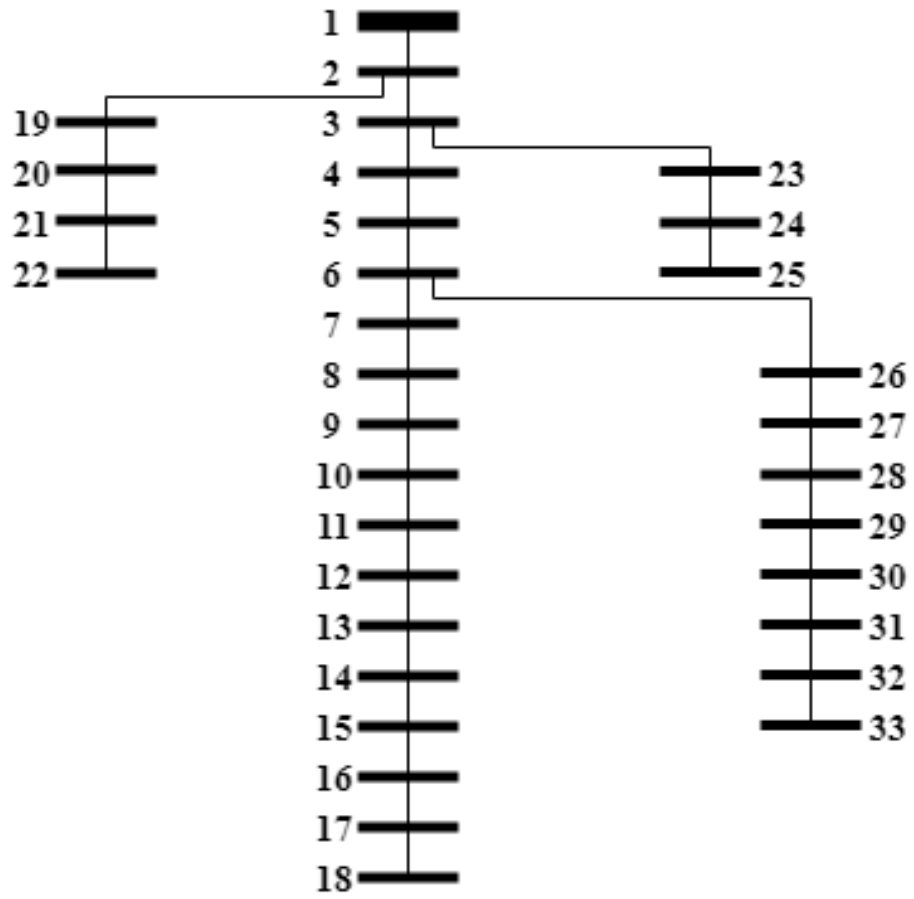
Figure A- 1. 33 Bus Radial Distributon Network

Table A- 1. *Bus Data*

Bus i	Type	Pd(kW)	Qd(kVar)
1	3	0	0
2	1	100	60
3	1	90	40
4	1	120	80
5	1	60	30
6	1	60	20
7	1	200	100
8	1	200	100
9	1	60	20
10	1	60	20
11	1	45	30
12	1	60	35
13	1	60	35
14	1	120	80
15	1	60	10
16	1	60	20
17	1	60	20
18	1	90	40
19	1	90	40
20	1	90	40
21	1	90	40
22	1	90	40
23	1	90	50
24	1	420	200
25	1	420	200
26	1	60	25
27	1	60	25
28	1	60	20
29	1	120	70
30	1	200	600
31	1	150	70
32	1	210	100
33	1	60	40

Table A- 2. Branch Data

From bus	To bus	r (Ω)	x (Ω)	b
1	2	0.0922	0.0470	0
2	3	0.4930	0.2511	0
3	4	0.3660	0.1864	0
4	5	0.3811	0.1941	0
5	6	0.8190	0.7070	0
6	7	0.1872	0.6188	0
7	8	0.7114	0.2351	0
8	9	1.0300	0.7400	0
9	10	1.0440	0.7400	0
10	11	0.1966	0.0650	0
11	12	0.3744	0.1238	0
12	13	1.4680	1.1550	0
13	14	0.5416	0.7129	0
14	15	0.5910	0.5260	0
15	16	0.7463	0.5450	0
16	17	1.2890	1.7210	0
17	18	0.7320	0.5740	0
2	19	0.1640	0.1565	0
19	20	1.5042	1.3554	0
20	21	0.4095	0.4784	0
21	22	0.7089	0.9373	0
3	23	0.4512	0.3083	0
23	24	0.8980	0.7091	0
24	25	0.8960	0.7011	0
6	26	0.2030	0.1034	0
26	27	0.2842	0.1447	0
27	28	1.0590	0.9337	0
28	29	0.8042	0.7006	0
29	30	0.5075	0.2585	0
30	31	0.9744	0.9630	0
31	32	0.3105	0.3619	0
32	33	0.3410	0.5302	0
21	8	2.0000	2.0000	0
9	15	2.0000	2.0000	0
12	22	2.0000	2.0000	0
18	33	0.5000	0.5000	0
25	29	0.5000	0.5000	0

APPENDIX B

POWER FLOW RESULT FROM MATPOWER

```
MATPOWER Version 7.0, 20-Jun-2019 -- AC Power Flow (Newton)

Newton's method power flow (power balance, polar) converged in 3 iterations.

Converged in 0.26 seconds
================================================================================
|     System Summary                                                           |
================================================================================

How many?                How much?          P (MW)           Q (MVAr)
---------------------    -------------------  -------------    ----------------
Buses            33      Total Gen Capacity   10.0             -10.0 to 10.0
Generators        1      On-line Capacity     10.0             -10.0 to 10.0
Committed Gens    1      Generation (actual)   3.9              2.4
Loads            32      Load                  3.7              2.3
  Fixed          32        Fixed               3.7              2.3
  Dispatchable    0        Dispatchable        -0.0 of -0.0    -0.0
Shunts            0      Shunt (inj)          -0.0              0.0
Branches         37      Losses (I^2 * Z)      0.20             0.14
Transformers      0      Branch Charging (inj)  -               0.0
Inter-ties        0      Total Inter-tie Flow  0.0              0.0
Areas             1

                          Minimum                      Maximum
                   -------------------------    --------------------------------
Voltage Magnitude   0.913 p.u. @ bus 18          1.000 p.u. @ bus 1
Voltage Angle      -0.50 deg   @ bus 18          0.50 deg   @ bus 30
P Losses (I^2*R)          -                       0.05 MW    @ line 2-3
Q Losses (I^2*X)          -                       0.03 MVAr  @ line 5-6

================================================================================
|     Bus Data                                                                 |
================================================================================
 Bus      Voltage          Generation             Load
  #   Mag(pu) Ang(deg)   P (MW)   Q (MVAr)   P (MW)   Q (MVAr)
----- ------- --------   --------  --------   --------  --------
    1  1.000    0.000*     3.92      2.44        -         -
    2  0.997    0.014       -         -        0.10      0.06
    3  0.983    0.096       -         -        0.09      0.04
    4  0.975    0.162       -         -        0.12      0.08
    5  0.968    0.228       -         -        0.06      0.03
    6  0.950    0.134       -         -        0.06      0.02
    7  0.946   -0.096       -         -        0.20      0.10
    8  0.941   -0.060       -         -        0.20      0.10
    9  0.935   -0.133       -         -        0.06      0.02
   10  0.929   -0.196       -         -        0.06      0.02
   11  0.928   -0.189       -         -        0.04      0.03
   12  0.927   -0.177       -         -        0.06      0.04
   13  0.921   -0.269       -         -        0.06      0.04
   14  0.919   -0.347       -         -        0.12      0.08
   15  0.917   -0.385       -         -        0.06      0.01
   16  0.916   -0.408       -         -        0.06      0.02
   17  0.914   -0.485       -         -        0.06      0.02
   18  0.913   -0.495       -         -        0.09      0.04
```

Figure B- 1. Power Flow Result from MATPOWER

```
19  0.997   0.004      -        -       0.09     0.04
20  0.993  -0.063      -        -       0.09     0.04
21  0.992  -0.083      -        -       0.09     0.04
22  0.992  -0.103      -        -       0.09     0.04
23  0.979   0.065      -        -       0.09     0.05
24  0.973  -0.024      -        -       0.42     0.20
25  0.969  -0.067      -        -       0.42     0.20
26  0.948   0.173      -        -       0.06     0.03
27  0.945   0.229      -        -       0.06     0.03
28  0.934   0.312      -        -       0.06     0.02
29  0.926   0.390      -        -       0.12     0.07
30  0.922   0.496      -        -       0.20     0.60
31  0.918   0.411      -        -       0.15     0.07
32  0.917   0.388      -        -       0.21     0.10
33  0.917   0.380      -        -       0.06     0.04
                    --------  --------  --------  --------
            Total:    3.92      2.44      3.72      2.30
```

```
================================================================================
|      Branch Data                                                             |
================================================================================
Brnch   From   To    From Bus Injection   To Bus Injection     Loss (I^2 * Z)
  #     Bus    Bus    P (MW)   Q (MVAr)    P (MW)   Q (MVAr)    P (MW)   Q (MVAr)
-----   -----  -----  -------- ---------   -------- ---------   -------- ---------
   1      1      2     3.92     2.44       -3.91    -2.43       0.012     0.01
   2      2      3     3.44     2.21       -3.39    -2.18       0.052     0.03
   3      3      4     2.36     1.68       -2.34    -1.67       0.020     0.01
   4      4      5     2.22     1.59       -2.20    -1.58       0.019     0.01
   5      5      6     2.14     1.55       -2.11    -1.52       0.038     0.03
   6      6      7     1.10     0.53       -1.09    -0.52       0.002     0.01
   7      7      8     0.89     0.42       -0.89    -0.42       0.005     0.00
   8      8      9     0.69     0.32       -0.68    -0.32       0.004     0.00
   9      9     10     0.62     0.30       -0.62    -0.29       0.004     0.00
  10     10     11     0.56     0.27       -0.56    -0.27       0.001     0.00
  11     11     12     0.52     0.24       -0.51    -0.24       0.001     0.00
  12     12     13     0.45     0.21       -0.45    -0.21       0.003     0.00
  13     13     14     0.39     0.17       -0.39    -0.17       0.001     0.00
  14     14     15     0.27     0.09       -0.27    -0.09       0.000     0.00
  15     15     16     0.21     0.08       -0.21    -0.08       0.000     0.00
  16     16     17     0.15     0.06       -0.15    -0.06       0.000     0.00
  17     17     18     0.09     0.04       -0.09    -0.04       0.000     0.00
  18      2     19     0.36     0.16       -0.36    -0.16       0.000     0.00
  19     19     20     0.27     0.12       -0.27    -0.12       0.001     0.00
  20     20     21     0.18     0.08       -0.18    -0.08       0.000     0.00
  21     21     22     0.09     0.04       -0.09    -0.04       0.000     0.00
  22      3     23     0.94     0.46       -0.94    -0.46       0.003     0.00
  23     23     24     0.85     0.41       -0.84    -0.40       0.005     0.00
  24     24     25     0.42     0.20       -0.42    -0.20       0.001     0.00
  25      6     26     0.95     0.97       -0.95    -0.97       0.003     0.00
  26     26     27     0.89     0.95       -0.88    -0.95       0.003     0.00
  27     27     28     0.82     0.92       -0.81    -0.91       0.011     0.01
  28     28     29     0.75     0.89       -0.75    -0.88       0.008     0.01
  29     29     30     0.63     0.81       -0.62    -0.81       0.004     0.00
  30     30     31     0.42     0.21       -0.42    -0.21       0.002     0.00
```

Figure B -1. Power Flow Result from MATPOWER (cont'd)

73

```
31    31    32    0.27    0.14    -0.27    -0.14    0.000    0.00
32    32    33    0.06    0.04    -0.06    -0.04    0.000    0.00
33    21     8    0.00    0.00     0.00     0.00    0.000    0.00
34     9    15    0.00    0.00     0.00     0.00    0.000    0.00
35    12    22    0.00    0.00     0.00     0.00    0.000    0.00
36    18    33    0.00    0.00     0.00     0.00    0.000    0.00
37    25    29    0.00    0.00     0.00     0.00    0.000    0.00
                                                  --------  --------
                                         Total:    0.203    0.14
```

Figure B -1. Power Flow Result from MATPOWER (cont'd)